

AUS DEM LEHRSTUHL FÜR INNERE MEDIZIN III
PROF. DR. WOLFGANG HERR
DER FAKULTÄT FÜR MEDIZIN
DER UNIVERSITÄT REGENSBURG

IN VITRO MODELLE ZUR UNTERSUCHUNG VON TRANSKRIPTIONSFAKTOREN

Inaugural – Dissertation
zur Erlangung des Doktorgrades
der Zahnmedizin

der
Fakultät für Medizin
der Universität Regensburg

vorgelegt von
Carolin Franziska Ponetsmüller

2022

AUS DEM LEHRSTUHL FÜR INNERE MEDIZIN III
PROF. DR. WOLFGANG HERR
DER FAKULTÄT FÜR MEDIZIN
DER UNIVERSITÄT REGENSBURG

IN VITRO MODELLE ZUR UNTERSUCHUNG VON TRANSKRIPTIONSFAKTOREN

Inaugural – Dissertation
zur Erlangung des Doktorgrades
der Zahnmedizin

der
Fakultät für Medizin
der Universität Regensburg

vorgelegt von
Carolin Franziska Ponetsmüller

2022

Dekan:	Prof. Dr. Dirk Hellwig
1. Berichterstatter:	Prof. Dr. Michael Rehli
2. Berichterstatter:	Prof. Dr. Wolfgang Dietmaier
Tag der mündlichen Prüfung:	21. April 2023

Table of Contents

1. Zusammenfassung	6
2. Introduction	8
2.1. Epigenetics and Regulation of Gene Expression	8
2.1.1. Chromatin Structure and Transcription	9
2.1.2. Transcription Factors	10
2.1.2.1. ETS-Family and Master Regulator PU.1	12
2.1.2.2. PU.1 and Interactions with other TFs	13
2.1.3. Histone Modification	14
2.1.4. ATP-dependent Chromatin Remodeling Complexes – in Detail the SWI/SNF-Family	15
2.2. Objectives	17
3. Material and Equipment	18
3.1. Laboratory Equipment	18
3.2. Consumables	19
3.3. Kits and Enzymes	20
3.4. Antibodies and Molecular Weight Standards	20
3.5. Chemicals	21
3.6. Solutions, Buffers and Antibiotic	22
3.7. Plasmid, Cell line and Bacteria	26
3.8. Oligonucleotides	27
3.9. Databases and Software	29
4. Methods	30
4.1. Cell Biological Methods	30
4.1.1. Cell Line Culture	30
4.1.1.1. Cell Line Culture Conditions and Passaging	30
4.1.1.2. Freezing and Thawing Cells	30
4.1.1.3. Assessing Cell Number and Viability	31
4.2. General Molecular Biology	31
4.2.1. Bacterial Culture	31
4.2.1.1. Production of LB-Amp Plates	31
4.2.1.2. <i>E. coli</i> Strain Cultivation and Glycerol Stock	31
4.2.2. Cloning Experiments	32

4.2.2.1.	Linearization of the Vector pEF6 for all Constructs	32
4.2.2.2.	Gel Extraction of DNA Fragments	32
4.2.2.3.	gBlocks Gene Fragments	33
4.2.2.4.	Gibson Assembly	33
4.2.2.4.1.	Transformation into <i>E. coli</i>	34
4.2.2.4.2.	Plasmid Isolation from <i>E. coli</i>	34
4.2.2.4.3.	Verification of Cloning Success	35
4.2.2.4.4.	1 % Agarose Gel Electrophoresis.....	36
4.2.3.	<i>In vitro</i> capped mRNA-Synthesis	36
4.2.3.1.	Plasmid DNA-Linearization and Purification	36
4.2.3.2.	<i>In vitro</i> Transcription	37
4.2.4.	Purification of mRNA	38
4.2.5.	Transfection of CTV-1 cells	39
4.2.5.1.	Electroporation of fusion protein mRNA in CTV-1 cell line	39
4.2.5.2.	Electroporation of Cas9/gRNA ribonucleoprotein (RNP) Complex .	40
4.2.5.3.	Fluorescent Cell Analysis	42
4.2.5.3.1.	Fluorescence Activated Cell Sorting.....	42
4.2.5.3.2.	Fluorescence Microscopy.....	43
4.2.5.4.	Amplification of Genomic DNA and Mutation Detection	43
4.2.5.4.1.	DNA-Isolation	43
4.2.5.4.2.	Amplification using Polymerase Chain Reaction	43
4.2.5.4.3.	DNA Cleanup	44
4.2.5.4.4.	Formation of Heteroduplexes for T7 Endonuclease digestion ...	44
4.3.	Protein Biochemical Methods	46
4.3.1.	Preparation of Whole Cell Lysates.....	46
4.3.2.	Sodium Dodecyl Sulfate Polyacrylamide Gel Electrophoresis	46
4.3.3.	Western Blot Analysis and Immunostaining.....	46
5.	Results.....	49
5.1.	Expression of Fluorescent Fusion Proteins in CTV-1 Cells	49
5.1.1.	Efficiency of Self-designed Constructs in Comparison to GFP	50
5.1.2.	Efficiency of different Linker Peptides - Flexible Linker vs. 2A-Peptide ...	51
5.1.2.1.	FACS Analysis of GFP transfected CTV-1 Cells	53
5.1.2.2.	Fluorescent Cell Imaging.....	53
5.2.	Genetic Manipulation in the Gene Locus of BRG1 in CTV-1 Cells	54
5.2.1.	Optimization of Electroporation Settings for CTV-1 Cells	55

5.2.2. Determination of Genome Targeting Efficiency via T7 Endonuclease Assay.....	56
5.2.3. Time-dependent Western Blot Analysis of transfected CTV-1 Cells	58
5.2.4. Growth and Morphology of CTV-1 Cells post Transfection.....	60
6. Discussion.....	63
6.1. CRISPR/Cas9-mediated BRG1 Targeting	64
6.2. Selection of Fluorescent Protein-PU.1 fusion.....	65
6.3. Perspectives	67
7. Summary	69
8. Appendix	70
8.1. List of Figures.....	74
8.2. List of Tables	75
9. Abbreviations.....	76
10. References	78
11. Acknowledgment	
12. Lebenslauf	

1. Zusammenfassung

Das Ergebnis der Transkription wird nicht nur durch die Wirkung eines einzelnen DNA-bindenden Transkriptionsfaktors (TF) bestimmt, sondern vielmehr durch das Zusammenspiel mehrerer TF und Enzyme untereinander und deren kombinatorischen Wechselwirkungen mit DNA (Lambert et al., 2018; Bondos und Tan, 2001; Howard und Davidson, 2004). Somit interagieren TF nicht nur mit DNA, sondern besitzen auch die Fähigkeit die Biologie anderer Proteine zu beeinflussen. Durch vorangegangene Arbeiten konnte gezeigt werden, dass der myeloische Master TF PU.1 mit einzelnen Enzymen der SWI/SNF-Familie, einschließlich BRG1 (codiert durch *SMARCA4*), interagieren kann (Minderjahn et al., 2020). Die genauen Mechanismen, wie die Interaktion zwischen PU.1 und BRG1 funktioniert und welche Auswirkungen es für die Biologie von PU.1 hat, ist noch nicht abschließend geklärt. Um dies genauer zu untersuchen, sind geeignete Modellsysteme notwendig, die unter anderem im Rahmen dieser Dissertation erarbeitet wurden. Als Modell diente dabei die bereits gut untersuchte T-Zell Leukämie Zelllinie CTV-1, welche PU.1 endogen nicht exprimiert. Zur visuellen Unterscheidung wurde im ersten Teil der Arbeit mittels Klonierungsexperimenten eine Auswahl an fluoreszierenden PU.1-Fusionsproteinen (FP) erstellt. Eine Validierung der Proteine erfolgte vorab über mRNA-Transfektionsexperimente. Um einen späteren Farbunterschied bei den beteiligten Proteinen zu generieren, wurden verschieden farbig fluoreszierende Fusionsproteine (FFP) designt und mittels Durchflusszytometrie (FACS) mit dem verstärkt grün fluoreszierenden Protein (enhanced Green Fluorescent Protein; eGFP) in Bezug auf Intensität und Stabilität verglichen. Diese Analysen ergaben die Überlegenheit von GFP gegenüber den selbst designten Konstrukten. Um aus sterischer Sicht ein möglichst stabiles FP zu generieren, wurden anhand weiterer FACS-Analysen verschiedene Linker Varianten analysiert und verglichen, wobei der flexible Linker (FL) gegenüber dem 2A-Peptid (P2A) zu bevorzugen ist. Der zweite Teil der Arbeit beschäftigt sich mit der Etablierung einer genetischen Manipulation im Genlocus BRG1 unter Zuhilfenahme des CRISPR (clustered regularly interspaced short palindromic repeats)/Cas9 Systems. Die On-target Effizienz wurde anhand eines T7-Endonuklease-I-Assay (T7EI) ermittelt und die BRG1-Proteinexpression in transfizierten CTV-1-Zellen mittels Western Blot (WB) unter Verwendung von

Anti-BRG1-Antikörpern analysiert. Sowohl die Abschätzung der genommodifizierenden Effizienz, als auch die BRG1-Proteinexpression nach CRISPR/Cas9-vermittelter Genom-Editierung sind vielversprechend. In Summe dient diese Arbeit der Erarbeitung von *in vitro* Modellen zur genaueren Untersuchung von Transkriptionsfaktoren und ihren assoziierten Proteinen und trägt somit zu einem besseren Verständnis des Zusammenspiels zwischen ihnen bei.

2. Introduction

A major principle in biology is the phenotype determination of individual cells in a multicellular organism. Though every cell possesses the same genes, there is a grand diversity of cell types – varying in cell morphology, function or other characteristics and properties. This can be explained by the fact that not every cell expresses all genes contained in the genome simultaneously (Evan, 1991). Thus, in each cell, only a limited number of genes are transcribed into RNA and protein, while other genes are switched off (Jannig and Knust, 2004). For this reason, a distinction is made between constitutive housekeeping genes, which are expressed ubiquitously, independently of cell-type and external influences, and cell type-specific genes, that are only transcribed in particular cells or at specific time points. The fine orchestration between all proteins and enzymes involved in gene regulation is crucial for the smooth execution of this complex process. The misregulation of gene expression programs can generate a wide range of diseases and the close association between neoplasia and aberrant regulation of gene expression is undeniable (Carroll, 2008; Lee and Young, 2013; Will et al., 2015). A better understanding of gene regulation and the correlation with diseases has become a key field of interest for biological and medical research.

2.1. Epigenetics and Regulation of Gene Expression

The regulation of transcription in eukaryotes occurs through the joint action of several components, including the basal transcriptional machinery, TFs and their interaction with *cis*-regulatory elements, as well as epigenetic mechanisms among others (Zhang et al., 2015). In 1942, the expression “epigenotype” was first described by Conrad Hal Waddington, focusing on the “causal interactions between genes and their products which bring the phenotype into being” (Waddington, 1942). Today, as we know well about DNA and its structure, when talking about epigenesis we mean the study of hereditary meiotic and/or mitotic modifications that result in phenotype changes, without entailing alterations in the DNA sequence (Egger et al., 2004; Waterland, 2006). Epigenetic modifications include covalent modifications of DNA bases and histone modifications, that alter chromatin structure, hence influencing DNA

accessibility for the transcription machinery and consequently regulating gene expression (Handy et al., 2011).

2.1.1. Chromatin Structure and Transcription

Chromatin structure and composition have a critical control function for transcription. Since chromatin is highly condensed during mitosis, DNA cannot be read and transcription is restricted to interphase when chromatin is uncoiled. Regarding the state of chromatin condensation and to differentiate active from inactive chromatin, the terms “euchromatin” and “heterochromatin” were introduced. Euchromatin describes the chromatin segments which uncoil and loosen up during interphase, whereas heterochromatin segments remain condensed throughout interphase. Due to the loosened chromatin structure in euchromatin, DNA is accessible to the proteins of the transcription machinery, thereby facilitating transcription (Jannig and Knust, 2004). In heterochromatic segments, DNA is less accessible and transcriptionally repressed (Morrison and Thakur, 2021). The smallest packaging unit of DNA is the nucleosome, which consists of a histone octamer (comprising of two copies of each of the four histone proteins H2A, H2B, H3, H4) surrounded by 1.65 spiral turns of genomic DNA, picturing a thread wrapped around a spool (Lawrence et al., 2016). Each nucleosome covers 146–147 base pairs (bp) and is connected to adjacent nucleosomes via linker DNA. During uncoiling, the linker DNA establishes the connection between the nucleosomes with the help of histone protein H1. By binding next to the nucleosome core particle, H1 helps to stabilize the nucleosome structure and allows the next higher-order chromatin structure (Izzo and Schneider, 2016). Nucleosome packaging in general limits the access to DNA for regulatory proteins by nature, yet it also offers the possibility of modulating chromatin structure and therefore regulating gene expression (Bell et al., 2011). The nucleosome filaments are increasingly condensed in several steps by additional proteins, commonly referred to as non-histone proteins. An important group of non-histone proteins are the High-Mobility-Group proteins (Janning and Knust, 2004). In eukaryotes, protein biosynthesis occurs in the cytoplasm. Hence, the 3`-5` DNA coding, antisense strand must be transcribed into mRNA, to enable transportation to the ribosomal enzymes. Since the growing strand is complementary to the noncoding template strand, the transcript has the same 5`-3` orientation as the strand complementary to the template. In general, three different RNA polymerases

are required for transcription to synthesize the different classes of RNA. Genes encoding polypeptides are predominantly transcribed by RNA polymerase II. However, eukaryotic polymerases cannot initiate transcription alone. For this purpose, TFs are necessary, which guide the way for the RNA polymerase (Buselmaier, 2003).

2.1.2. Transcription Factors

Even though a gene is located in euchromatin and transcription is therefore possible in principle, its expression is subject to strict regulatory control. Cell type-specific transcriptional regulation of gene expression is inter alia depending on the coordinated action of TFs (Choukrallah and Matthias, 2014; Voss and Hager, 2014). As seen in **figure 2.1**, TFs are proteins, that recognize and bind in a sequence-specific manner to signal sequences (motifs) within regulatory gene segments (Lambert et al., 2018). These segments function as *cis*-acting DNA elements that interact with *trans*-acting TFs. If *cis*-acting DNA elements lead to an inhibition of transcription, they are called silencers, whereas *cis*-elements that lead to an amplification of transcription and are not part of promoters, are called enhancers (Maniatis et al., 1987).

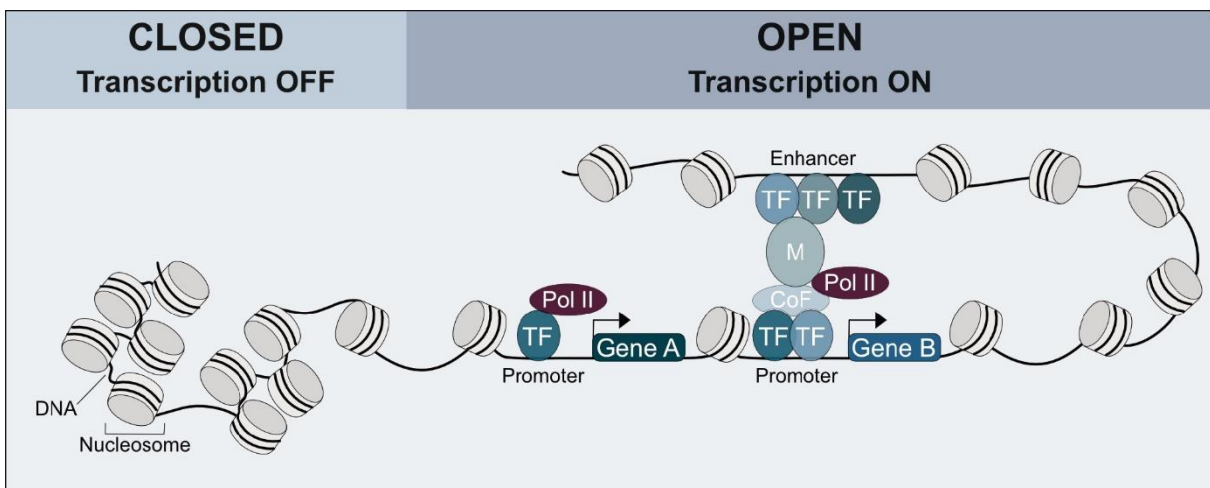


Figure 2.1: Transcription initiation and its associated proteins

When DNA is closed, no transcription can be initiated. Uncoiled chromatin enables TFs to bind in a sequence-specific manner to *cis*-acting DNA elements, like promoters and enhancers. They can either guide the way for Polymerase II directly to signal sequences on DNA or cooperate with other enzymes such as mediators and cofactors to assemble the transcription initiation complex. (Transcription factor (TF), RNA polymerase II (Pol II), Mediator (M), Cofactor (CoF); graphic illustration by Leiz et al., 2021).

The interplay of TFs with regulatory DNA segments like enhancers or upstream activator elements plays a key role in the controlling of gene expression and influences transcription rate. This affects the transcriptional outcome, either in a positive manner (activation) or through an inhibiting effect (repression) (Latchman, 1997).

According to their specificity for the regulation of gene activity, general TFs (GTFs) are distinguished from specific or regulatory TFs (RTFs). GTFs along with the RNA-polymerase form the basal transcription apparatus and GTFs activities were linked to numerous basic activities. They help RNA polymerase II to recognize the TATA-box region of promoters and by binding to the DNA, GTFs function as a platform, onto which the polymerase can bind. Hence, they help to initiate transcription from the core regions of promoters and to form the transcription initiation complex (Reese, 2003; Orphanides et al., 1996). The presence of GTFs is the minimum requirement for the initiation of transcription and is responsible for a minor, basal transcriptional activity of all genes of a gene class (Pierce, 2012; Reese, 2003). RTFs, on the other hand, are often cell-specific and selectively regulate a gene or a group of genes. They are capable of amplifying manyfold the only minor basal transcription of certain genes by binding to *cis*-regulatory elements close or afar from the promoter sequence and thus enable cells to selectively control their expression patterns. They interact with the transcription machinery as either activator or repressor and can intervene in a regulating way in the recruitment and organization of the initiation complex. This can essentially determine the transcription frequency (Müller-Esterl, 2018). TFs usually possess different functional parts. This includes the conserved DNA-binding domain (DBD) as well as the less conserved trans-activating domain (TAD). In many cases, TFs also contain domains that serve to dimerize with the same or different TFs (Janning and Knust, 2004). Originally described in 1989, TFs can be classified into major TF families, according to their recognition motifs. The most common structural motifs in DBDs are the Cys2-His2 zinc finger (C2H2-ZF), basic helix-loop-helix, basic leucine zipper, Homeodomain and nuclear hormone receptor (Johnson and McKnight, 1989). The correct binding of a TF to DNA is important and obligatory to modulate transcription, though alone it is not sufficient. TFs have to interact with co-regulators by forming broad networks of cooperating TFs or even with the RNA polymerase itself to influence DNA interaction (Davidson, 2006; Carroll, 2008).

2.1.2.1. ETS-Family and Master Regulator PU.1

One of the larger TF-families is the erythroblast transformation-specific (ETS) family, comprising 27 human ETS-genes, which are divided into 11 subfamilies (Gutierrez-Hartmann et al., 2007). ETS-family TFs are typified by a highly conserved DNA-binding domain of about 85 amino acids, the so-called ETS-domain and are found in all multicellular organisms. The ETS-domain comprises a conserved winged helix-turn helix structure and is composed of three alpha-helices and four-stranded anti parallel beta sheets (Donaldson et al., 1996, Sharrocks et al., 1997; Weirauch and Hughes, 2011). They positively and/or negatively regulate the expression of a variety of cellular genes by binding to a purine-rich 5'-GGA(A/T)-3' core sequence in cooperation with other TFs and co-factors (Sharrocks, 2001). ETS-family members are key regulators of immune cell development, proliferation and differentiation. They play a superior role in angiogenesis, hematopoiesis and neuronal development and are transcriptional targets of many signaling pathways (Bartel et al., 2000; Schober et al., 2005). One subfamily of the ETS-family is the SPI TF family, including PU.1, SPIB and SPIC. The pioneer TF PU.1 is encoded by the *SPI1* gene and works as a transcriptional activator in hematopoietic cell lineages. It is a key regulator in hematopoietic tissues with high levels of expression in the monocytic, macrophage and B lymphocytic lineages and early stages of T-cell development (Rothenberg et al., 2019; Klemsz et al., 1990). PU.1 serves as a versatile master regulator and so-called pioneer factor. Pioneer TFs have the essential ability of binding within closed and condensed heterochromatin domains, thereby providing chromatin accessibility for additional TFs (Soufi et al., 2015). Although PU.1 can remodel chromatin and recruit additional cell type-specific TFs to their "unmasked" DNA binding sites, PU.1 is not a classical pioneer TF in the conventional sense, since *in vitro* experiments showed that PU.1 is not able to bind to nucleosome-bound targets (Minderjahn et al., 2020; Kadoch and Crabtree, 2015). Next to the ETS-domain, PU.1 contains three additional domains, including a glutamine-rich domain and an N-terminal acidic domain, which are both engaged in transcriptional activation (see **figure 2.2**). For protein-protein interaction, PU.1 possesses a so-called PEST-domain (rich in proline, glutamic acid, serine and threonine), which plays a role in monocyte-specific gene expression. Nevertheless, the exact domain function is depending on the target genes and the differentiation stage of the cell. Post-translational modification of the PU.1 protein takes place by

phosphorylation at serine 41 in the N-terminal acidic domain and at serines 142 and 148 in the PEST domain which in turn leads to increased activity (Burda et al., 2010; Nishiyama et al., 2004). The misregulation of PU.1 is often associated with cancer (Takei and Kobayashi, 2019). Overexpression of PU.1 is related to hematological malignancies and PU.1 mutations seem to contribute to the development of acute myeloid leukemia (Klemsz et al., 1990; Mueller et al., 2002; Moreau-Gachelin et al., 1988).

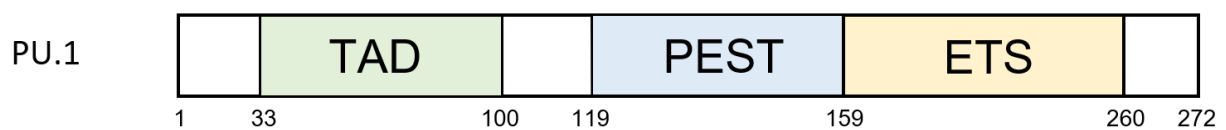


Figure 2.2: TF PU.1 and its domains

This figure illustrates the schematic structure of the TF PU.1. Depicted is the TAD-domain (transactivating domain), consisting of an acidic and glutamine-rich domain, the PEST-domain for protein-protein interaction and an ETS-domain, which is necessary for DNA-binding (adapted from Rothenberg et al., 2019).

2.1.2.2. PU.1 and Interactions with other TFs

The detailed modes behind the binding mechanisms between TFs like PU.1 and other TFs are not entirely understood yet, but multiple ways of interaction have been identified. Due to the inability of many TFs to bind to DNA as a single, monomeric protein, they can interact with other TFs through direct protein-protein contact, to build functional protein-level dimers, trimers or tetramers. Interactions can also be solely DNA-facilitated in the absence of stable protein-protein contacts, which means that only in the presence of DNA, TF complexes can be built. This allows a greater number of TF pairs than direct protein-protein interactions. DNA-mediated interactions of TFs often lead to an alteration in DNA shape, which can result in increased affinity for the binding of further TFs. Another important mechanism is the so-called indirect cooperativity. This term explains a competition between TFs and nucleosomes, therefore the word cooperativity can be deceptive (Morgunova and Taipale, 2017). Although PU.1 can work as a pioneer factor to open chromatin sites for other TFs, it can also function as a collaboration-dependent partner in binding complexes and is

able to interact with various regulatory factors. Beginning with GTFs like TFIID and the TATA-Box binding Protein TBP, early hematopoietic transcription factors like GATA-binding protein 2, erythroid factors like the GATA-binding protein 1, non-erythroid factors like the CCAAT enhancer-binding protein C/EBP α and PU.1 coactivator c-Jun (Burda et al., 2010; Gupta et al., 2010; Zhang et al., 1999). These protein-protein complexes and interactions can modify the overall transcriptional activity of PU.1 and modulate cell fate decisions. The TF PU.1 combined with its transcriptional partners can regulate the expression of a minimum of 3000 genes expressed in hematopoietic cells. These include e.g. cell-surface proteins, cytokines and their respective receptors (Gangenhalli et al., 2005; Burda et al., 2010).

2.1.3. Histone Modification

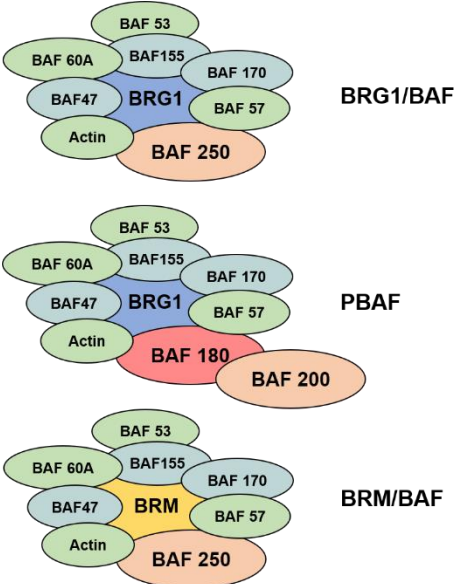
As already mentioned above, transcriptional regulation is primarily controlled by the binding of the transcriptional machinery proteins to the core promoter sequences on the DNA. Due to the tight packaging of DNA, some structures cannot interact with the transcription machinery (Janning and Knust, 2004). DNA accessibility is facilitated by two different mechanisms: by covalent histone modification using histone-modifying enzymes and chromatin remodeling, using ATP-dependent nucleosome remodelers. This allows dynamic access to regulatory regions by altering the chromatin architecture and exposing DNA regions for transcriptional regulation (Hargreaves and Crabtree, 2011, Wang et al., 2007). Chemical histone modifications can affect the binding affinity between DNA and nucleosomes and can cause the transition from open, transcriptionally active chromatin to condensed, transcriptionally inactive chromatin. Therefore, posttranslational modification (PTM) of histone proteins can change chromatin properties. Histone PTM describes the addition or removal of small chemical molecules like methyl, phosphoryl and acetyl groups to amino acids at the N-terminal histone tails, catalyzed by histone-modifying enzymes (Zhang et al., 2015; Janning and Knust, 2004). This can either directly lead to a change in the nucleosome architecture or support the binding of specific TFs. Amino acid acetylation, catalyzed by histone acetyltransferases, results in neutralization of the positive charges of histones. This in turn leads to a looser binding to the negatively charged phosphate residues of DNA and is consequently related to transcriptional activity and chromatin accessibility. In contrast, histone deacetylases have a negative impact on transcriptional activity

(Muchardt and Yaniv, 2001). Histone methylation of lysine and arginine, catalyzed by the histone methyltransferase, can either have activating or repressing effects depending on the amino acid modified (Morrison and Thakur, 2021).

2.1.4. ATP-dependent Chromatin Remodeling Complexes – in Detail the SWI/SNF-Family

Chromatin remodelers are large, multi-component complexes comprising multiple subunits, which use the energy of ATP hydrolysis to promote nucleosome translocation by weakening the interaction between DNA and histone core particles (Erdel et al., 2011; Muchardt and Yaniv, 2001). Chromatin remodelers can be classified into subfamilies according to their subunit configuration, which include SWI/SNF, ISWI, CHD and INO80 chromatin remodeling complexes (Wu et al., 2019). Recruitment of remodeling complexes is mediated by chromatin-associated signals like histone PTMs or target proteins like pioneer TFs (Erdel et al., 2011). Chromatin remodeling complexes can either activate or repress, by facilitating the binding of TFs. The SWI/SNF family, named after its phenotypic alterations “mating-type switch” and “sucrose non-fermentable”, represents a well-studied group of chromatin remodeling complexes (Jancewicz et al., 2019; Peterson and Herskowitz, 1992). Originally described in *S. cerevisiae*, each complex comprises 8-15 subunits (Cairns et al., 1994). Two large subfamilies of SWI/SNF remodelers are the BRG1/BRM-associated factor complex (BAF) and the polybromo BRG1-associated (PBAF) factor complex (Kadoch and Crabtree, 2015; Phelan et al., 1999). As seen in **figure 2.3**, each SWI/SNF complex employs one of the two related but mutually exclusive catalytic ATPase subunits, BRM/SMARCA2 (encoded by the *SMARCA2* gene) or BRG1/SMARCA4 (encoded by the *SMARCA4* gene), which both harbor DNA and protein interaction modules (Wu et al., 2017). BAF complexes also contain the low-specificity DNA binding subunit BAF250, the tumor suppressor gene BRCA1 and an AT-rich interactive domain, comprising ARID1A (BAF250A) and ARID1B (BAF250B), whereas in PBAF complexes solely BRG1 as ATPase enzyme, the polybromo protein (BAF180), ARID2 (BAF200) and BRD7 (bromodomain-containing 7) subunits are present (Reisman et al., 2009; Muchardt and Yaniv, 2001; Wilson and Roberts, 2011; see **table 2.1**). ATP-dependent chromatin remodeling complexes can alter the locus of nucleosomes by either repositioning nucleosomes through sliding the histone octamer along the

DNA or completely ejecting them (Tang et al., 2010). SWI/SNF remodeling complexes are also able to cooperate with tissue-specific TFs by either activating or suppressing genes. ATP-dependent SWI/SNF chromatin remodeling enzymes are key regulators in lineage-specific differentiation and play a leading role in cancerous growth, since many types of human cancers show alterations in genes encoding the SWI/SNF remodeling complexes. Subunit encoding genes are altered in over 20 % of malignant neoplasia (Alver et al., 2017; Masliah-Planchon et al., 2015). BRG1 mutations are associated with the tumorigenesis of certain malignancies like medulloblastoma, lung cancer or acute leukemia, proving that BRG1 acts as tumor suppressor protein (Clapier et al., 2017; Wilson and Roberts, 2011; Parsons et al., 2011; Reisman et al., 2003).



Subunits	Associated genes
BRG1	SMARCA4
BRM	SMARCA2
BAF250A	ARID1A
BAF250B	ARID1B
BAF200	ARID2
BAF180 (polybromo protein)	PBRM1
BRCA1	BRCA1 gene
BRD7	BRD7 gene

Figure 2.3: Different domains of BAF and PBAF complexes

BAF complexes comprise either BRG1 or BRM as ATPases, whereas PBAF only employs BRG1 (illustration adapted from Reisman et al., 2009).

Table 2.1: Selection of SWI/SNF subunits in mammals

Shown is a selection of SWI/SNF complex subunits with their encoding genes (table adapted from Reisman et al., 2009).

2.2. Objectives

Minderjahn et al. showed that PU.1 interacts with members of the SWI/SNF family of chromatin remodeling complexes, including BRG1 (*SMARCA4*) among others. This interplay is mediated by the acidic domain of the TAD, suggesting that an absence of BRG1 could have a reducing effect on PU.1 binding (Minderjahn et al., 2020).

Suitable model systems are needed to furtherly investigate the interaction between the non-classical pioneer TF PU.1 and the SWI/SNF ATPase BRG1 and the manner it influences the biology of PU.1. A selection of FFPs is designed and experiments of their respective efficiencies are carried out, to visualize the way the enzymes interact and to see, whether a subsequent restructuring of the proteins involved occurs. Validation of the proteins is performed beforehand via mRNA transfection and FACS analysis. The second part of this work aims at establishing genetic manipulation in the gene locus of BRG1 using CRISPR/Cas9-technology. The genetic manipulation serves to insert HDR-mediated degrons later on or to perform further manipulations. As a model, the CTV-1 cell line, a human T cell leukemia cell line, that does not endogenously express PU.1, was chosen.

3. Material and Equipment

3.1. Laboratory Equipment

Autoclave	Walter, Geislingen, Germany
Axiovert 40 c Microscope	Zeiss, Jena, Germany
Biofuge Pico	Heraeus, Hanau, Germany
Centrifuges	Heraeus, Hanau, Germany; Eppendorf, Hamburg, Germany; Thermo Fischer Scientific, Waltham, USA
Cryo Container	Nalgene, Sigma-Aldrich, Taufkirchen, Germany)
Cryocube	Eppendorf, Hamburg, Germany
Electrophoresis equipment	Bio-Rad, Munich, Germany
EVOS cell Imaging System	Thermo Fisher Scientific, Waltham, USA
Fluorescence cell Imager Zoe	Bio-Rad, Munich, Germany
Flow Cytometers (FACSymphony A5, LSRFortessa)	Becton Dickinson, Heidelberg, Germany
Gene Pulser Xcell Electroporation System	Bio-Rad, Munich, Germany
Heatblock	Eppendorf, Hamburg, Germany
HERAcell 240i CO ₂ Incubator	Thermo Fisher Scientific, Waltham, USA
Incubators	Heraeus, Hanau, Germany
Incubation shaker MaxQ 8000	Thermo Fisher Scientific, Waltham, USA
Laminar air flow cabinet	Heraeus, Hanau, Germany
Master cycler Nexus gradient	Eppendorf, Hamburg, Germany
myECL Imager	Thermo Fisher Scientific, Waltham, USA
NanoDrop Spectrophotometer (ND-1000, 2000)	PeqLab, Erlangen, Germany
Neon Transfection System	Thermo Fisher Scientific, Waltham, USA
Picofuge	Heraeus, Hanau, Germany
PTC-200 Gradient Thermal Cycler	MJ-Research/Biometra, Oldendorf, Germany
Qubit 2.0 Fluorometer	Thermo Fisher Scientific, Waltham, USA
Standard Power Packs Biometra P25	Analytik Jena, Jena, Germany
TapeStation 4150	Agilent Technologies, Böblingen, Germany

Thermomixer	Eppendorf, Hamburg, Germany
UVP PCR Workstation	Analytik Jena, Jena, Germany
Vortex Genie	Scientific Industries, New York, USA
Waterbath	Memmert, Schwabach, Germany
Whatman Fastblot B44	Biometra, Göttingen, Germany

3.2. Consumables

Assay tubes (Qubit)	Invitrogen, Thermo Fisher Scientific, Waltham, USA
Cell culture flasks and pipettes	Eppendorf, Hamburg, Germany
Cell culture plates (6-, 24-well)	Eppendorf, Hamburg, Germany
Centrifuge tubes (15, 50, 225 ml)	Falcon, Heidelberg, Germany
Cryo tubes	Nunc, Wiesbaden, Germany
Electroporation cuvettes (0.4 cm)	PeqLab, Erlangen, Germany
Hemocytometer C-CHIP (NI)	VWR International GmbH, Darmstadt, Germany
Immobilon-P PVDF membrane	Merck Millipore, Darmstadt, Germany
Loading tips (TapeStation)	Agilent Technologies, Böblingen, Germany
Micro test tubes low binding (0.5, 1.5, 2.0 ml)	Sarstedt, Nümbrecht, Germany; Eppendorf, Hamburg, Germany
Multiwell cell culture plates and tubes	Eppendorf, Hamburg, Germany
Optical Tube, 8x strips and caps	Agilent Technologies, Böblingen, Germany
PCR plate Twin.tec 96-well	Eppendorf, Hamburg, Germany
PCR SoftTubes, 0.2 ml	Thermo Fisher Scientific, Waltham, USA
Petri dishes	Falcon, Heidelberg, Germany
QIAfilter Midi Cartridges	Qiagen, Hilden, Germany
Whatman 3MM CHR	GE Healthcare, Chalfont St. Giles, UK

3.3. Kits and Enzymes

Kits

Alt-R CRISPR-Cas9 System	IDT, Coralville, USA
Alt-R Genome Editing Detection Kit	IDT, Coralville, USA
dNTPs	Thermo Fisher Scientific, Waltham, USA
DNeasy Blood & Tissue Kit	Qiagen, Hilden, Germany
Gibson Assembly Master Mix	NEB, Frankfurt, Germany
KAPA HiFi HotStart ReadyMix	Roche, Mannheim, Germany
mMESSAGE mMACHINE T7 Ultra Kit	Thermo Fisher Scientific, Waltham, USA
Monarch DNA Gel Extraction Kit	NEB, Frankfurt, Germany
Monarch PCR & DNA Cleanup Kit	NEB, Frankfurt, Germany
Monarch Plasmid Miniprep Kit	NEB, Frankfurt, Germany
Neon Transfection System 10 µL Kit	Thermo Fisher Scientific, Waltham, USA
Plasmid Plus Midi Kit	Qiagen, Hilden, Germany
Plasmid Midi Kit	Qiagen, Hilden, Germany
Qubit dsDNA HS Assay Kit	Thermo Fisher Scientific, Waltham, USA
QIAquick Gel Extraction Kit	Qiagen, Hilden, Germany
RNeasy Midi and Mini Kit	Qiagen, Hilden, Germany

Enzymes

All Enzymes used for DNA digestion were stored at -20 °C. The restriction endonucleases were either purchased from New England Biolabs (NEB, Frankfurt, Germany) or Roche (Mannheim, Germany).

3.4. Antibodies and Molecular Weight Standards

Antibodies for Western Blot

Anti-BRG1	Abcam, Cambridge, UK
Anti-Actin	Sigma-Aldrich, Taufkirchen, Germany

Molecular Weight Standards

GeneRuler 1 kb Plus DNA Ladder	Thermo Fisher Scientific, Waltham, USA
Precision Plus Protein Kaleidoscope	Bio-Rad, Munich, Germany

3.5. Chemicals

1 M NaOH	Carl Roth, Karlsruhe, Germany
β -Mercaptoethanol 50mM	Gibco, Thermo Fisher Scientific, Waltham, USA
Acrylamide (ROTIPHORESE 30 %)	Carl Roth, Karlsruhe, Germany
Agarose	Carl Roth, Karlsruhe, Germany
Ammonium Persulfate	Sigma Aldrich, Taufkirchen, Germany
Ampicillin	Carl Roth, Karlsruhe, Germany
Aqua	Braun, Melsungen, Germany
Bacto Tryptone	BD Biosciences, Heidelberg, Germany
Bacto Yeast	BD Biosciences, Heidelberg, Germany
Bovine Serum Albumin (BSA)	Sigma Aldrich, Taufkirchen, Germany
Phosphate Buffered Saline (PBS)	Gibco, Thermo Fisher Scientific, Waltham, USA
ECL Prime Western Blotting System	Sigma-Aldrich, Taufkirchen, Germany
EDTA 0.5 M (pH 8.0)	Merck Millipore, Darmstadt, Germany
Fetal Calf Serum (FCS)	Sigma Aldrich, Taufkirchen, Germany
Formaldehyde 16 %, methanol-free	Thermo Fisher Scientific, Waltham, USA
Glycerol	Merck Millipore, Darmstadt, Germany
Glycine	Carl Roth, Karlsruhe, Germany
Glycogen	Invitrogen, Thermo Fisher Scientific, Waltham, USA
KCl	Merck Millipore, Darmstadt, Germany
L-Alanyl-L-Glutamine	Merck Millipore, Darmstadt, Germany
MgCl ₂	Merck Millipore, Darmstadt, Germany
NaBut	Sigma-Aldrich, Taufkirchen, Germany
NaCl	Merck Millipore, Darmstadt, Germany
NaHCO ₃	Merck Millipore, Darmstadt, Germany
Non-Essential Amino Acid Solution	Sigma Aldrich, Taufkirchen, Germany

Nonfat-dried milk	Sucofin, Vienna, Austria
Nonident P-40 (NP-40)	Roche, Mannheim, Germany
Opti-MEM	Gibco, Thermo Fisher Scientific, Waltham, USA
Penicillin-Streptomycin (10,000 U/ml)	Gibco, Thermo Fisher Scientific, Waltham, USA
Phenol:Chloroform:Isoamylalkohol 25:24:1	Invitrogen, Thermo Fisher Scientific, Waltham, USA
PhosSTOP EASYpack	Roche, Mannheim, Germany
ReBlot Plus Mild 10X	Merck Millipore, Darmstadt, Germany
ROTI-GelStain	Carl Roth, Karlsruhe, Germany
RPMI 1640	Gibco, Thermo Fisher Scientific, Waltham, USA
Sodium Dodecyl Sulfate (SDS)	Sigma Aldrich, Taufkirchen, Germany
Sodium Pyruvate	Sigma Aldrich, Taufkirchen, Germany
Tetramethylethylendiamin (TEMED)	Sigma Aldrich, Taufkirchen, Germany
Tris(hydroxymethyl)aminomethane (Tris)	Thermo Fisher Scientific, Waltham, USA
Trypan Blue Solution 0.4 %	Sigma Aldrich, Taufkirchen, Germany
Tween 20	Sigma Aldrich, Taufkirchen, Germany
UltraPure Distilled Water (DNase/RNase free)	Invitrogen, Thermo Fisher Scientific, Waltham, USA
Vitamin Solution	Sigma Aldrich, Taufkirchen, Germany

3.6. Solutions, Buffers and Antibiotic

Frequently used Solutions

Bacterial culture

SOC-medium:	20 g (2 %)	Bacto Tryptone
	5 g (0.5 %)	Yeast extract
	0.6 g (10 mM)	NaCl
	0.2 g (3 mM)	KCl
	Ad 1000 ml	H ₂ O
	adjust pH to 7.5, autoclave	

Supplements:	10 ml (10 mM)	MgCl ₂ (1 M)
	10 ml (10 mM)	MgSO ₄ (1 M)
	10 ml (20 mM)	Glucose (2 M)
LB-Medium:	10 g	Bacto Tryptone
	10 g	NaCl
	5 g	Yeast extract
	Ad 1000 ml	H ₂ O
	Autoclave	
LB-Amp Plates:	15 g	Agar
	1000 ml	LB-Medium
	100 µg/ml	Ampicillin
1% Agarose Gel Electrophoresis		
TAE (50X):	242.3 g (2 M)	Tris
	20.5 g (250 mM)	NaOAc/HOAc (pH 7.8)
	18.5 g (0.5 M)	EDTA (pH 8.0)
	Ad 1000 ml	H ₂ O
	store at RT	
DNA loading dye (5X):	500 µl (50 mM)	Tris, 1 M (pH 7.8)
	500 µl (1 %)	SDS (20 %)
	4 ml (40 %)	Glycerol (100 %)
	1 ml (50 mM)	EDTA, 0.5 M (pH 8.0)
	10 g (1 %)	Bromphenol blue
	Ad 10 ml	H ₂ O
	store at 4 °C	
1 % Agarose Gel:	0.6 g (1 %)	Agarose
	60 ml	1X TAE

heat the slurry in a microwave until agarose is completely dissolved, cool down to 50 °C and add 5 µl ROTIGel Statin

DNA ladder working dilution

20 µl	5X DNA loading Dye
20 µl	1 kb Plus DNA Ladder
ad 100 µl	H ₂ O
store at 4 °C	

Whole Cell Lysates

2X SDS Sample Buffer:

10 ml (150 mM)	Tris, 1.5 M (pH 6.8)
6 ml (1.2 %)	SDS (20 %)
30 ml	Glycerol
15 ml	β-mercaptoethanol
1.8 mg	Bromophenol blue
Ad 100 ml	H ₂ O
aliquot in 10 ml stock solution and store at -20 °C, store working solution at 4 °C	

10 % Separating Gel

4 ml	H ₂ O
3.3 ml	Acrylamide (30 %)
2.5 ml	Seperating Gel Buffer
100 µl	SDS (10 %)
100 µl	APS (10 %)
4 µl	TEMED

5 % Stacking Gel:

5.5 ml	H ₂ O
1.3 ml	Acrylamide (30 %)
1 ml	Stacking Gel Buffer
80 µl	SDS (10 %)
80 µl	APS (10 %)
8 µl	TEMED

Separating Gel Buffer:	90.83 g (1.5 M) Ad 500 ml	Tris/HCl (pH 8.8) H ₂ O
Stacking Gel Buffer:	30 g (0.5 M) Ad 500 ml	Tris/HCl (pH 6.8) H ₂ O
SDS (10 %):	100 g (10 %) Ad 1000 ml adjust pH to 7.2	SDS H ₂ O
Ammonium Persulfate (APS):	1 g (10 %) Ad 10 ml	APS H ₂ O
Laemmli Buffer (5X):	15 g (40 mM) 216 g (0.95 M) 15 g (0.5 %) Ad 3000 ml	Tris Glycine SDS H ₂ O
TBS (10X):	45.8 g (100 mM) 175.5 g (1.5 M) Ad 2000 ml	Tris/HCl (pH 8.0) NaCl H ₂ O
Western Blot		
Anode Buffer A:	36.3 g (0.3 M) 200 ml (20 %) Ad 1000 ml	Tris Methanol H ₂ O
Anode Buffer B:	3.03 g (25 mM) 200 ml (20 %) Ad 1000 ml	Tris Methanol H ₂ O
Cathode Buffer C:	5.20 g (4 mM)	ε-Amino-n-caproic acid

	200 ml (20 %)	Methanol
	Ad 1000 ml	H ₂ O
Washing Buffer (1X TBST):	100 ml	TBS (10X)
	1 ml (0.05 %)	Tween 20
	Ad 1000 ml	H ₂ O
Blocking Buffer:	3.0 g (3 %)	nonfat dried milk
	100 ml	TBS

Other Buffers

2:1 Buffer	NEB Frankfurt, Germany
3:1 Buffer	NEB, Frankfurt, Germany
CutSmart Buffer	NEB, Frankfurt, Germany
IDTE Buffer	IDT, Coralville, USA
Monarch DNA Elution Buffer	Qiagen, Hilden, Germany
TE Buffer	Qiagen, Hilden, Germany

Antibiotic

Ampicillin	Roth, Karlsruhe, Germany
------------	--------------------------

3.7. Plasmid, Cell line and Bacteria

Plasmid

<i>pEF6/V5-His Topo</i>	Thermo Fisher Scientific Waltham, USA
-------------------------	---------------------------------------

Cell Line

CTV-1

Human acute myeloid leukemia (DSMZ ACC 40)

Bacteria

DH10β

Escherichia coli
(F⁻ *mcrA* Δ(*mrr-hsdRMS-mcrBC*)
φ80*lacZ*Δ*M15* Δ*lacX74* *recA1* *endA1*
araD139 Δ (*ara-leu*)7697 *galU*
galk λ⁻ *rpsL*(Str^R) *nupG*)

3.8. Oligonucleotides

gBlocks Gene Fragments

All gBlocks gene fragments were synthesized and high-affinity chromatography purified from Integrated DNA Technologies (IDT, Coralville, USA).

PU.1-mNeon

```
GATCCactataggagaccaagctggctaggaagcttggtagccgagctcggatccgccaccATGTTGCAAGCCTGCAAGATGGAAGGATTCCCTT
GGTCCCgcctccgctcTGAGGATCTTGTCCCTACGACACTGATCTCTATCAGAGGCAGACACACGAATATTATCCATACCT
GTCCAGTGATGGGGAGTCACATTCAGATCATTACTGGGATTTTCATCCGCATCACGTCCATTCTGAGTTTGAAAGCTTCGCA
GAAAACAATTTTACCGAGCTGCAAAGCGTGCAACCCCTCAACTTCAACAGCTTTATCGGCATATGGAGCTCGAGCAGATG
CATGGCTTGATACACCGATGGTGCTCCACATCCGTCCTTGGGCCATCAAGTGTCTACCTCCGAGGATGTGTTTGCAA
TACCCTTCTTGTCTCCGGCGCAACCCAGCTCCGACGAGGAAGAAGGAGAGAGGCAATCCCCGCCATTGGAAGTGAGTGA
CGGGGAAGCCGACGGTCTTGAGCCGGGTCCCggcctcCTTCTGGCGAAACTGGCAGCAAGAAAAAGATCAGACTCTATC
AGTTTTTGCTTGATCTCTCCCGCAGCGGTGACATGAAAGACAGTATTTGGTGGGTGGATAAAAGATAAAGGGACGTTCCAGT
TTTCATCCAAGCATAAAGAAGCTCTCGCTCACAGGTGGGGTATCCAGAAGGGTAATCGCAAAAAGATGACTTATCAGAAGAT
GGCACGAGCGCTTAGGAACATATGGCAAAACAGGCGAAGTTAAAAAAGTGAAAAAGAAGCTTACGTACCAATTTAGTGGGGA
GGTCTTGGGTGGGGTGGACTTGGCGGAGCGGAGACATCCACCCACACAATGTCTGTGGACAGTTCACTTCCGTCACCGA
ATCAGCTGTCCAGCCCTCATTGGGATTCGACGGTCTCCCTGGGCGAATGGTATCAAAGGGGGAAGAAGATAATATGGCG
TCTTTGCCGGCGACGCATGAACTTCATATATTCGGAAGTATCAATGGTGTAGACTTCGACATGGTCCGGCCAGGGTACCGGG
AACCCEAATGACGGATATGAGGAGCTGAACCTCAAGAGTACAAAGGGTGACCTTCAGTTTAGTCCATGGATATTGGTACCC
CACATCGGATACGGTTTTTACCAATACCTGCCATATCCAGATGGCATGTCTCCTTTCCAGGCAGCCATGGTAGACGGGTCT
GGGTATCAGGTTTCATCGCACTATGCAGTTTGAAGACGGAGCATCACTCACGGTTAACTATAGATATACTTACGAAGGCTCAC
ATATAAAAGGGGAGGCTCAGGTTAAGGGTACTGGTTTCCCGGCAGATGGACCAGTGATGACAAACTCAATTGACAGCCGCA
GACTGGTGTGCGCAGCAAGAAAACCTACCCTAACGATAAAACCATCATTCTACCTTTAAGTGGTCTTATACAACGGGGAACG
GAAAGAGATACAGAAGTACGGCCCGCACACATACACTTTCGCGAAGCCAATGGCAGCCAATTACTTGAAGAACCAACCCA
TGTATGTGTTCCGAAAAACCGAATTGAAGCACAGTAAGACCGAGTTGAACTTCAAAGAGTGGCAGAAAGGCTTCACAGACG
TCATGGGTATGGATGAGCTTTACAAGGCTAGTGCTACGATGTGGTCCCACCCCAAGTTTCGAAAAAGGTGGCGGGCTCAGGG
GGTGGATCGGTGGCGGGAGCTGGTCACATCCTCAATTCGAGAAAAACGAGCCGGGCGGATTATAAAGATCACGATGGTGA
TTATAAAGACCATGATATCGATTATAAAGATGACGATGATAAACGCTCATGATctagaggcccggttcgaaggtaagcctatccctaaccctc
cctcggctcctgattctacggtaccggtTCTAG
```

PU.1-mScarlet

```
ATGCTGCAGGCTTGTAAGATGGAGGGGTTCCCTCTTGTACCGCCACCCTCCGAGGACTTGGTACCTTACGATACAGATTTG
TATCAACGACAGACCCACGAATACTACCCGTACTTGTCTCAGACGGGGAGTCCCACAGTGATCACTACTGGGACTTTTCA
```

CCCCATCATGTCCACTCCGAATTCGAGTCATTCGCCGAAAATAACTTCACAGAGCTTCAAAGTGTACAACCCCCACAGTTGC
AACAACTCTACCGACACATGGAACCTTGAGCAGATGCACGTTCTCGATACGCCCATGTTCCCCCTCATCCCTCATTGGGCC
ATCAGGTATCATATCTGCCGAGAATGTGTTGCAGTATCCGAGCTTGAGCCCGGCGCAGCCTTCTAGTGATGAGGAGGAAG
GAGAGAGACAGTCTCCTCCCCCTTGAGGTAAGTGATGGCGAAGCTGATGGTCTGGAGCCTGGGCCCGTTTGTCTGCCAGG
CGAAACAGGGAGCAAAAAAAAAAATTAGATTGTATCAGTTTTTGTCTGGATTTGTCTCCGGAGTGGGGATATGAAAGATAGCATA
TGGTGGGTGGACAAGGATAAGGGGACATTTCAATTCAGCTCTAAGCACAAGGAGGCGCTCGCGCATAGATGGGGAAATCA
AAAGGGTAATCGCAAGAAGATGACTTACCAAAAGATGGCACGGGCTTGAGGAATTATGGAAGACAGGAGAAGTAAAAAA
AGTGAAGAAGAAGCTGACTTACCAATTTAGTGGCGAGGTAAGTCTCGGTAGAGGGGGCCTGGCTGAACGCCGACATCCTCCTC
ACacaatgtctgtgactctcattgacctagcccaaatcaactcagttctccgagcctcggtctgatggattgcttggacggATGGTCTCTAAGGGGGAAGCTGTAA
TTAAGGAATTTATGAGGTTTAAAGTGCATATGGAAGGTAGTATGAACGGTCACGAGTTGAAAATTGAAGGGGAAGGTGAAG
GACGACCGTACGAGGGCACTCAGACAGCCAAGCTCAAAGTACGAAGGGGGGCCCGCTTCCCTTCTCTGGGATATTCTC
AGCCCCAGTTTATGTACGGGTCTCGCGCTTTACAAAACACCCAGCGGATAATCCAGACTATTATAAGCAGTCTTTCCCG
AGGGCTTTAAGTGGGAGCGGTTATGAACCTTCAAGACGGCGGTGCTGTGACGGTAACACAAGATACTCTCTTGAGGAC
GGGACATTTGATCTACAAGGTAAGCTCAGAGGTACAAATTTCTCTCTGATGGGCCAGTGTGCAAAAAGAAGACAATGGGG
TGGGAAGCCAGCACTGAGAGACTGTACCCAGAAGATGGAGTTCTTAAAGGAGACATTAATAATGGCCCTGAGGCTTAAGGAT
GGCGGGCGATACCTTGAGATTTCAAGACAACGTACAAAGCGAAAAAGCCGGTGCAAAATGCCAGGAGCTTACAACGTTGAT
AGAAAGCTTGATATCACATCACATAATGAGGACTATACCGTCGTCGAGCAGTACGAACGCTCCGAAGGCAGACACAGTACG
GGAGGTATGGATGAGCTGTATAAAGCGTCAGCAACTATGTGGTACACCCACAATTCGAAAAAGGGCGGTGGCTCAGGAGG
CGGGAGCGGAGGTGGATCCTGGTCCCACCTCAATTTGAAAAGACTTCCCGAGCAGATTATAAGGACCATGACGGCGACT
ACAAGGACCATGACATCGATTACAAGGATGATGATGACAAGCGGAGTTG

P2A-eGFP

actatagggagaccgaagctggctaggttaagcttggtagcagctcgatccgaccATGTTGCAAGCCTGTAAGATGGAGGGGTTTCCGCTCGTCC
CTCCACCTAGTGAAGACTTGGTACCGTATGACACCGACCTTTACCAACGACAAAACCCATGAATATTACCCTTATTTGAGCTC
CGACGGGGAGAGCCACTCCGACCACTACTGGGATTTTACCCACACCAGTTTATTCTGAGTTTGAATCATTGCGGAAAA
TAATTTACCGAGCTCCAGTCCGTACAGCCTCCGCAGCTTCAACAGTTGTATAGACATATGGAACCTCGAGCAAAATGCACGTA
TTGGATACGCCTATGGTTCACCACATCCCTCCCTCGGACATCAAGTCTTATCTTCCACGCATGTGCCTCCAATACCCGA
GTTTGTACCTGCCAGCTAGTTCGACGAGGAAGAAGGCCGAGCCAGAGCCCGCCCTTGAGGTTGATGATGGCGA
AGCCGACGATTGGAACCGGGGCCGGTCTGCTTCTGGCGAAACCGGAAGCAAGAAGAAGATTGCTCTTTATCAGTTTC
TGCTCGATTTGCTTAGGAGCGGGGACATGAAAGATTCTATTTGGTGGGTGGATAAAGGAACTTTTCAATTTTCAAG
TAAGCACAAAGGAGCTCTTGCGCACAGATGGGGCATTGAGAAAGGAAACCGGAAAAAAATGACATACCAAAAGATGGCTAG
AGCGTTGAGAAATTACGGGAAGACTGCGAAGTGAAGAAAGTAAAAAAGAAACTCACTTATCAGTTTTCTGGCGAGGTAAGT
GGGCGAGGGGGCTCGCCGAACGACGGCACCCCGCCGACGGCAGCGGAGCAACAACTTCTCATTGCTTAAAGCAAGCAG
GGGACGTGGAGGAAACCCAGGACCAACTTCAATGGTTAGTAAAGGTGAGGAGTTGTTTACTGGGTAGTCCCAATTTCTTG
TTGAGCTTGACGGAGACGTTAACGGGCATAAGTTCTCAGTGTACAGGAGAGGGGGAGGGTGTGCCACGTACGGGAAGCT
GACCCTGAAGTTTATTTGACACCACGGGTAAACTCCCTGTGCCCTGGCCTACCCTGGTGACGACACTTACCTATGGTGCCA
ATGCTTTTCTCGGTATCCGGACCATATGAAGCAGCATGATTTTTCAAATCAGCCATGCCTGAAGGCTATGTACAGGAGCGG
ACTATCTTTTAAAGACGATGGTAACTACAAGACCGGGCAGAGGTGAAATTTGAGGGAGACACCCTGGTTAACCAGGATC
GAGCTGAAAGGGATCGACTTCAAAGAGGACGGTAACATTTGGGGCATAAGCTCGAGTATAATTACAACAGTACATAATGTG
TACATTTAGCCAGACAAGCAAAAAAATGGGATAAAGTTAACTTCAAGATAAGACATAATATCGAAGACGGGTCCCGTCAAT
TGGCAGACCATTATCAGCAGAACACGCCCATAGGGGATGGACCAGTGTCTTGCCTGATAATCACTACCTGTCAACACAAA
GTGCTTTGTCTAAGGACCCGAACGAAAACGAGACCATATGGTACTGCTTGTAGTTTGTAACTGCAGCAGGTATCACCCCTCG
GTATGGACGAACTGTACAAGGCCAGTCTACGATGTGGAGTACCCGCAATTCGAGAAGGGAGGTGGATCTGGTGGCGG
GTCCGGAGGTGGTCTGGTCTACCCCCAGTTTAAAAAAGTACGAGAGCAGATTATAAGGATCAGATGGCGACTATAA
AGACCACGATATAGACTACAAAGATGATGACGATAAAGATCTTGATctagagggcccggttcgaaggaagcctatccctaaccctctcctgctc
tcgattctacgctaccggt

Flexiblelinker-eGFP

actatagggagaccgaagctggctaggttaagcttggtagcagctcgatccgaccATGTTGCAAGCCTGTAAGATGGAGGGGTTTCCGCTCGTCC
CCCCTCCGAGTGAGGACTTGGTCCCCTATGACACTGATCTGTATCAGCGACAGACACAGTACTACCCATACCTCTCCT
CTGACGGCGAGAGCCATTCTGATCATTACTGGGACTTCCATCCCACCATGTTCACTCCGAATTTGAGAGCTTTGCGAAAA
TAATTTTACCGAATTTCAATCCGTGCAACCACCGCAACTGCAGCAACTCTATAGACATATGGAGCTGGAACAGATGCACGTT
CTTGATACGCCTATGGTCCCACCCACCCGCTCTGAGGACCAAGTTAGCTATTTGCCTAGGATGTGTCTCCAATATCCGT
CATTTGCCCGCACAACTTCCCTCCGATGAGGAGGAGGGAGAGCGCCAGAGCCCCCTCTCGAGGTCTCTGATGGGGA
AGCTGATGGCTCGAACCAGGGGGCCGATTGCTTCCGGGCGACCCGGTCAAAGAAGAAGATACGACTGTACCAGTTT
CTGCTCGACCTGCTTCCGAGCGGGGACATGAAGGACAGCATTGGTGGGTAGATAAAGACAAAGGAACATTTCAATTTCTCT
TCTAAACACAAAGAAGCCTTGGCACACCGGTGGGGTATTCAAAAAGGCAATCGCAAGAAAATGACCTATCAGAAGATGGCC
CGGGCGCTGCGAAACTACGGTAAAACAGGGGAAGTGAAGAAAGTAAAAAAGAACTGACATACCAGTTCTCAGGTGAGGTT
CTGGGAAGGGGAGGGCTGGCGGAGCGAAGACATCCGCTCACACAATGCTGTAGATAGTTTCTTCCCTCACCTACCA
GCTTTTCTCTCCTAGCCTTTGGGTTTACCGGCTGCCCGGTAGGATGGTATCAAAGGGTGAAGAACTTTTCACTGGTGTCTG
CCCTATTCTGGTTGAGCTCGATGGCGATGTCAATGGACATAAATTTCCGTTTCCGGTGAAGGGGAAGGGGATGCTACATA
CGGGAAGCTGACGTTGAAATTCATCTGCACCACAGGCAACTTCTGTACCATGGCCGACGCTTGTGACTACGCTCACCTA
TGGTGTACAATGTTTCTAGATACCCCGATCATGAAACAGCAGCAGCTTCTTCAAGAGCGCAATGCCAGAGGGGTACGT
TCAGGAGAGGACCAATTTTTTCAAAGACGACGGAACCTATAAACTAGGGCTGAGGTAAGTTTTGAGGGGGATACGCTGGT
AAATCGGATCGAACTGAAAGGCATTGACTTTAAGGAGGATGGGAATATACTGGGGCATAAAGTCCGAGTACAACATAAATAGC

CATAATGTTTATATTATGGCAGACAAGCAGAAGAACGGAATTAAGTTAATTTAAGATCCGCCATAATATTGAAGATGGATC
 TGTACAGTTGGCCGACCAATTACCAACAGAATACCCCAATAGGAGATGGGCCAGTCTTGCTGCCTGACAAATCATTATCTCTCC
 ACCCAGAGCGCGTTGAGTAAGGACCCGAATGAGAAGCGGGACCACATGGTTCTTCTCGAGTTCGTGACGGCGGCAGGCAT
 CACCCTCGGTATGGACGAACTCTATAAGGCTAGTGCTACGATGTGGAGTCATCCTCAGTTCGAAAAGGGAGGCCGGGTCCG
 GTGGTGGCTCTGGCGGAGGATCTTGGAGTCACCCACAGTTCGAGAAGACCAGTCGGGCTGATTATAAGGACCACGATGGA
 GATTACAAAGACCATGACATAGACTACAAAGATGACGATGATAAGCGCTCTTGAtctagagggccccggttcgaaggaagcctatccctaac
 cctctcctcggctctcgattctacggtaccggt

Amino acid sequence of P2A: (GSG)ATNFSLLKQAGDVEENPGP

Amino acid sequence of FL: TMSVDSSLPSPNQLSSPSLGFDFGLPGR

CRISPR/Cas9 gRNA and Primers for T7 Endonuclease Assay

gRNA	GGGTCGAGACTGGAATGTCTG
T7ea_SMARCA4_FWD	CATGGGACAGAGCAGGGAAGGCACG
T7ea_SMARCA4_REV	CTCCCAGGCACAAGTCCACCTGCAG

3.9. Databases and Software

Benchling	https://www.benchling.com/
BLAST	https://blast.ncbi.nlm.nih.gov/Blast.cgi
Image J	https://imagej.nih.gov
Microsoft Office 365	Microsoft Corporation, Redmond, USA
PubMed	www.ncbi.nlm.nih.gov/entrez
SnapGene Viewer v2.8.2 GSL	Biotech LLC, Chicago, USA
TapeStation A.01.05 (SR1)	Agilent Technologies, Böblingen, Germany
UCSC Genome Browser	www.genome.ucsc.edu
UniProt	http://www.uniprot.org

4. Methods

4.1. Cell Biological Methods

If not otherwise indicated, all cell centrifugation steps were carried out at 300 x g for 8 min at 4 °C.

4.1.1. Cell Line Culture

4.1.1.1. Cell Line Culture Conditions and Passaging

Cells were cultured in RPMI 1640 (Gibco, Thermo Fisher Scientific, Waltham, USA) containing 10 % heat-inactivated FCS (inactivation at 56 °C for 20 min), sodium pyruvate (1 mM), L-glutamine (2 mM), antibiotics (50 µg/ml streptomycin and 50 U/ml penicillin), 2 ml vitamins, 50 µM β-mercaptoethanol and non-essential amino acids. CTV-1 cells were cultured in non-treated cell culture flasks and incubated at 37 °C, 5 % CO₂ and with 95 % relative humidity. Every 2-3 days, cells were counted, split and reseeded into fresh medium. For passaging, CTV-1 cells were centrifuged and washed with Phosphate Buffered Saline (PBS) at 4 °C. After centrifugation, the suspension was poured into new cell culture flasks with fresh medium, diluted 1:10.

4.1.1.2. Freezing and Thawing Cells

Before reaching confluency, 5-10 x 10⁶ cells were harvested and suspended in 1 ml freezing medium, containing 900 µl RPMI 1640, 10 % FCS, supplements and 100 µl DMSO. After transferring the cells into cryotubes, they were stored in isopropanol-filled cryo containers at -80 °C for 24 h. For long-term storage, the cryotubes were kept in liquid nitrogen at -196 °C.

The nitrogen-cooled cells were thawed and directly transferred into prewarmed medium containing 20 % FCS. To remove freezing medium residues, the cells were centrifuged and resuspended in fresh medium containing 10 % FCS. The first medium exchange was performed one day after thawing.

4.1.1.3. Assessing Cell Number and Viability

Cell number and viability were determined microscopically using Trypan blue exclusion assay. The cell suspension was diluted 1:2 with Trypan blue Solution 0.4 % and counted under the microscope in a Neubauer hemocytometer. Living cells stain only faintly, while dead cells appear dark. Living cells were counted and the concentration C was calculated using the following formula with N being the average number of living cells:

$$C \left[\frac{\text{viable cells}}{\text{ml}} \right] = N \times \text{dilution factor} \times 10^4$$

4.2. General Molecular Biology

4.2.1. Bacterial Culture

4.2.1.1. Production of LB-Amp Plates

The LB-Medium (see **section 3.6**) was mixed with the agar and boiled up several times under constant stirring. After cooling down the slurry to 50 °C, the appropriate antibiotic was added. The mixture was then poured into 10 cm petri dishes, again cooled down and stored at 4 °C.

4.2.1.2. *E. coli* Strain Cultivation and Glycerol Stock

For overnight growth, *Escherichia coli* (*E. coli*) strains were streaked out on LB-Amp plate with an inoculating loop and cultured at 37 °C.

Single ampicillin-resistant bacterial colonies were picked and inoculated into liquid LB-Medium (containing 100 µg/ml ampicillin) and incubated overnight with shaking at 200 rpm at 37 °C.

For permanent storage, bacterial cultures were stored in 20 % glycerol (600 µl liquid culture mixed with 200 µl of 80 % glycerol) placed in cryotubes at -80 °C.

4.2.2. Cloning Experiments

4.2.2.1. Linearization of the Vector pEF6 for all Constructs

For all subsequent constructs, the plasmid pEF6/V5-His Topo was used. For vector linearization, the plasmid was digested with restriction enzymes and substances were added as follows (see **table 4.1**).

Table 4.1: Linearization of the vector pEF6/V5-His Topo (amount for 1 reaction)

Reagents	Amount
DNA (pEF6/V5-His Topo plasmid)	1 µg
Buffer 2.1	3 µl
Xba1	1.5 µl
BamH1	1.5 µL
H ₂ O	ad 30 µl

The mixture was digested at 37 °C for 1 h. To heat inactivate the enzymatic activity, a 20 min long incubation at 65 °C followed. After digestion, the mixture was loaded onto a 1 % Agarose Gel (see **section 4.2.2.4.4**).

4.2.2.2. Gel Extraction of DNA Fragments

Under UV illumination, the DNA band containing the desired fragment was cut out. Purification was carried out via gel extraction, using the Monarch DNA Gel Extraction Kit (NEB, Frankfurt, Germany) according to the manufacturer's instructions.

After purification, the DNA was eluted in 10 µl Elution Buffer (EB) and the concentration was measured via NanoDrop spectrophotometer.

4.2.2.3. gBlocks Gene Fragments

The used gBlocks Gene Fragments are customized, double-stranded DNA fragments of up to 3000 bp in length and the industry standard for CRISPR/Cas9-mediated genome editing. All gBlocks were synthesized from Integrated DNA Technologies (IDT, Coralville, USA). The used amount of gBlocks Gene Fragments was 1000 ng. In order to reach a concentration of 10 ng/μl, 100 μl TE-Buffer were added, briefly vortexed and incubated at 50 °C for 20 min.

4.2.2.4. Gibson Assembly

In 2009, Daniel G. Gibson and colleagues were first to describe an exonuclease-based molecular cloning method, which allows a seamless assembly of multiple DNA fragments in a single reaction, regardless of fragment length. Gibson Assembly employs three enzymatic activities in one reaction. The enzymatic mixture consists of a 5' exonuclease, a DNA polymerase and a thermophilic DNA ligase. The exonuclease activity generates long overhangs, the DNA polymerase activity incorporates nucleotides to fill in the gaps and the ligase activity combines the DNA of adjacent segments (Gibson et al., 2009).

For Gibson Assembly reaction, gBlocks Gene Fragments were specifically designed to the DNA site of interest with an overlapping DNA sequence (see **section 3.8**).

The fragment mass was calculated using the following formula, with l being vector length and m vector mass:

$$m_{fragment} [ng] = \frac{3 \times m_{vector} [ng] \times l_{fragment} [bp]}{l_{vector} [bp]}$$

For the assembly, a three-fold molar excess of insert fragments and 50 ng linearized pEF6/V5-His Topo plasmid DNA were used. For reaction setup see **table 4.2**.

**Table 4.2: Gibson Assembly reaction setup
(amount for 1 reaction)**

Reagents	Amount
Linearized pEF6/V5-His Topo plasmid	50 ng
gBlocks Gene Fragments	3x molar excess
Gibson Assembly Master Mix 2X (NEB)	10 μ l
H ₂ O	Ad 20 μ l

After a 1 h long incubation at 50 °C, 2 μ l of the Gibson Assembly reaction were transformed into chemically competent *E. coli*.

4.2.2.4.1. Transformation into *E. coli*

For transformation into *E. coli* bacteria, 50 μ l of *DH10 β* (chemically competent *E. coli* cells) were thawed on ice. After adding 2 μ l of Plasmid ligation, the mixture was gently resuspended and incubated on ice for 30 min. After heat-shocking cells at 42 °C for 90 s, they were cooled on ice for 2 min until 250 μ l of prewarmed SOC medium were added. The suspension was incubated with shaking at 37 °C for 60-90 min, before 50-100 μ l of transformed bacteria were distributed on LB-Amp plates and incubated overnight at 37 °C.

4.2.2.4.2. Plasmid Isolation from *E. coli*

For plasmid isolation from *E. coli* (< 100 μ g) the Monarch Plasmid Miniprep Kit and to isolate larger amounts of DNA (\geq 100 μ g) the Qiagen Midi Kit were used according to manufacturer's instructions.

For plasmid isolation smaller 100 μ g, 2 ml of bacterial culture was pelleted by centrifugation for 30 s. After the supernatant was discarded, the pellet was resuspended in 200 μ l Plasmid Resuspension buffer and vortexed. To lyse the cells, a 200 μ l Plasmid Lysis Buffer was added and inverted several times. Neutralization of the lysate was reached by adding 400 μ l of Plasmid Neutralization Buffer and inverting the tube gently. The lysate was clarified by spinning the tube for 5 min at 16,000 x g. The supernatant was carefully transferred to the spin column and centrifuged for 1 min,

the flow-through was discarded. Afterwards, 200 µl of Plasmid Wash Buffer 1 were added and centrifuged for 1 min. Subsequently, 400 µl of Plasmid Wash Buffer 2 were added onto the spin column and again centrifuged for 1 min. The DNA was eluted in 30 µl EB.

For plasmid isolation greater 100 µg, 30 ml of bacterial culture was pelleted by centrifugation at 3,500 rpm for 15 min at 4 °C and the supernatant was discarded. The pellet was completely resuspended in 4 ml P1-Buffer. After resuspension, 4 ml of P2-Buffer were added and inverted several times. Next, a 5 min long incubation followed and 4 ml of pre-chilled P3-Buffer were added, inverted and transferred into the Qiafilter Midi Cartridge. After letting the mixture incubate for 10 min, the lysate was carefully filtered through the Qiafilter Midi Cartridge into the Qiagen-tip 100. The Qiagen-tip was washed twice with 10 ml QC-Buffer. In order to elute the DNA, 5 ml QF-Buffer were added and filtered into 3.5 ml of 2-Propanol (100 %). The Eluate was centrifuged at 4,500 x g for 45 min at 4 °C. The supernatant was discarded and the pellet was washed with 2 ml ethanol (70 %) and again centrifuged at 4,500 x g for 15 min at 4 °C. The supernatant was discarded and the pellet was air-dried for 10 min. The DNA pellet was resolved in 100 µl of TE-Buffer and the concentration was determined via NanoDrop spectrophotometer.

4.2.2.4.3. Verification of Cloning Success

To verify the correct base sequence, restriction enzyme digestion in combination with Sanger Sequencing was used. Suitable restriction enzymes (NEB, Roche) were identified via SnapGene Viewer. For digestion, the following reagents in **table 4.3** were added.

Table 4.3: Restriction enzyme digestion

Reagents	Amount
Plasmid DNA	1 µg
Restriction Enzyme	10-20 U
Buffer 2.1	1 µl
H ₂ O	ad 10 µl

The plasmid DNA was digested at 37 °C for 1 h and its quality and size were assessed by 1 % Agarose Gel electrophoresis (see **section 4.2.2.4.4**). To ensure the correct nucleotide sequence, the constructs were sequenced by GeneArt (Thermo Fisher) using the Sanger Sequencing Method with vector-specific primers. Sequence analysis was carried out via the online platform benchling.

4.2.2.4.4. 1 % Agarose Gel Electrophoresis

To prepare a 1 % agarose gel solution, the required amount of 1 % agarose was mixed with Electrophoresis Buffer 1X TAE in a ratio of 1g/100ml and heated in a microwave until the agarose was completely dissolved and no streaks were visible. After the gel was transferred into a gel tray and has set, it was placed into an electrophoresis chamber and covered with 1X TAE. Before loading the samples into the gel slots, 5X DNA loading dye was added in a ratio of 4:1. For size comparison, 5 µl of DNA ladder working dilution (see **section 3.6**) was applied to the gel. Depending on the desired resolution and DNA fragment size, gels were run at 90-120 V for 30 to 60 min. For imaging, myECL Imager was used.

4.2.3. *In vitro* capped mRNA-Synthesis

4.2.3.1. Plasmid DNA-Linearization and Purification

Prior to *in vitro* mRNA-synthesis, the plasmid DNA was linearized with restriction endonuclease digestion and purified using phenol/chloroform extraction and ethanol precipitation. The plasmid including the inserted DNA was digested with appropriate restriction endonucleases. For 20 µg of DNA, 10-20 U of the enzyme were digested in 8 µl of the appropriate buffer. H₂O was added up to 80 µl and the mixture was incubated for 1 h at 37 °C. To purify linearized plasmid DNA, one volume of Phenol:chloroform:isoamyl alcohol (25:24:1) was added to the sample and vortexed for 20 sec. The mixture was then centrifuged at 13,000 rpm for 5 min at RT. The upper aqueous phase containing the DNA was carefully removed and transferred to a fresh tube. To remove the residual phenol, the sample was precipitated twice with equal volumes of chloroform and centrifuged at 13,000 rpm for 2 min at RT. After transferring the aqueous phase to a new tube, DNA was precipitated with the 0.5-fold volume of 5

M NH₄OAc and a 2.5-fold volume of Ethanol (100 %) at -80 °C for 1 h. To pellet the DNA, the sample was centrifuged at 13,000 rpm for 30 min at 4 °C. The supernatant was removed and the pellet was washed with 150 µl of pre-chilled Ethanol (70 %). Another centrifugation at 13,000 rpm for 2 min at 4 °C followed. After the supernatant was removed, the DNA pellet was air-dried for 10 min at RT and was subsequently resuspended in 20 µl RNase/DNase-free H₂O. The concentration was determined using the NanoDrop Spectrophotometer and successful linearization was verified by 1 % agarose gel electrophoresis. Purified, linearized plasmids were stored at 4 °C.

4.2.3.2. *In vitro* Transcription

To generate poly-adenylated and capped mRNA from purified, linearized DNA plasmids, the mMessage mMachine T7 ultra reaction Kit from Ambion (Thermo Fischer Scientific, Waltham, USA) was used according to the manufacturer's instructions.

Until completely dissolved, the T7 2X NTP/ARCA and the 10X T7 Reaction Buffer were thawed at RT and the T7 2X NTP/ARCA was stored on ice afterwards. The remaining components were added at RT according to the following listed order (see **table 4.4**).

Table 4.4: *In vitro* mRNA synthesis reaction setup (amount for 1 reaction)

Reagents	Amount
T7 2X NTP/ARCA	10 µl
10X T7 Reaction buffer	2 µl
Linear DNA	1 µg
T7 Enzyme Mix	2 µl
Nuclease-free H ₂ O	ad 20 µl

The reaction was gently mixed and incubated for 2 h in a heat block at 37 °C. In order to digest the remaining DNA, 1 µl of TURBO DNase was added and a 20 min long incubation at 37 °C followed. After incubation and before Poly(A)Tailing was added, 1 µl of the reaction was saved as a control sample.

To generate a Poly(A)-Tail, the following components were pipetted to the reaction above (see **table 4.5**).

**Table 4.5: Poly(A)-Tailing reaction setup
(amount for 1 reaction)**

Reagents	Amount (µl)
mMessage mMachine T7 Ultra Reaction	20
H ₂ O (nuclease-free)	36
5X PAP-Buffer	20
25 mM MnCl ₂	10
ATP solution	10
E-PAP Enzyme	4

The reaction was gently mixed and incubated for 1 h at 37 °C, yielding a poly (A)-tail around 50-100 bases.

4.2.4. Purification of mRNA

To purify the synthesized transcripts, the Qiagen RNeasy Mini Kit (Hilden, Germany) was used according to the manufacturer's instructions. After 350 µl of RLT Buffer and 250 µl of Ethanol (100 %) were added to the mMessage mMachine T7 Ultra reaction, the sample was directly mixed and pipetted onto a spin column. Centrifugation of the sample at 11,000 rpm for 30 sec at RT followed and the flow-through was discarded. The spin columns were washed once with 500 µl RW1 and twice with 500 µl RPE with the same centrifugation settings listed above. To dry the pellet and to remove residual EtOH, another centrifugation with the empty column for 1 min at 13,000 rpm at RT was carried out. The transcripts were eluted in 50 µl nuclease-free H₂O and placed on ice.

The concentration of the mRNA transcripts was determined via NanoDrop spectrophotometer. To ensure transcript's quality, the Agilent 4150 TapeStation with RNA ScreenTape was used. The transcripts were frozen immediately in aliquots at -80 °C until further use.

4.2.5. Transfection of CTV-1 cells

4.2.5.1. Electroporation of fusion protein mRNA in CTV-1 cell line

To validate the quality of the protein, transfection via electroporation with the Gene Pulser Xcell (Bio-Rad) and an attached measurement via FACS analysis was carried out. The day before transfection, CTV-1 cells were counted and cultivated in a new cell culture flask with 20 ml RPMI growth medium (incl. 10 % FCS) per 1×10^6 cells. On the day of transfection, Opti-MEM and RPMI 1640 without phenol red (1 ml/ 1×10^6 CTV-1 cells) were prewarmed at 37 °C in a 6-well plate. Cells were counted using a Neubauer hemocytometer and for each time point, 1×10^6 cells were centrifuged with 1,000 rpm for 10 min at RT.

After discarding the supernatant, the pellet was washed once with 10 ml RPMI 1640 and once with 10 ml Opti-MEM at 1,200 rpm for 8 min at RT. The supernatant was again removed and the pellet was resuspended in 200 μ l Opti-MEM for each electroporation. Different amounts of mRNA were pipetted into a 4 mm cuvette, depending on the pre-measured concentration of the samples, and 200 μ l of cell suspension were added. To avoid any bubbles, the cuvettes were carefully tapped a few times and directly placed into the electroporation chamber of the Gene Pulser Xcell™ (Bio-Rad) and pulsed with the following settings (see **table 4.6**).

**Table 4.6: Gene Pulser Xcell
Electroporation settings**

Waveform	3 Square wave
Voltage	400
Square wave timing	5 ms
Cuvettes	4 mm

After electroporation, cells were immediately transferred into the prewarmed growth medium and incubated at 37 °C for up to 24 h.

4.2.5.2. Electroporation of Cas9/gRNA ribonucleoprotein (RNP) Complex

Transfection of the Cas9/gRNA ribonucleoprotein (RNP) complex was carried out with the Neon Transfection System (Thermo Fischer Scientific, Waltham, USA). To maximize the transfection outcome, the 24-well optimization protocol for suspension cell lines was used (see **table 8.1a/b**; Invitrogen, Thermo Fisher).

For transfection of the RNP complex, cells with the lowest passage number possible were used and the culture medium and flask were changed one day before electroporation. The crRNA oligos (10 nm) were ordered at IDT (Coralville, USA) and resuspended in 50 μ l IDTE Buffer to obtain a concentration of 200 μ M. The resuspended RNA oligos were stored at -20 °C. For the crRNA:tracrRNA duplex, the crRNA and tracrRNA were mixed as shown in **table 4.7** according to IDT instructions in equimolar concentrations to a final duplex concentration of 44 μ M.

Table 4.7: Formation of the crRNA:tracrRNA Duplex

Reagents	Amount (μ l)
200 μ M Alt-R CRISPR-Cas9 crRNA	2.2
200 μ M Alt-R CRISPR-Cas9 tracrRNA	2.2
Nuclease-Free IDTE Buffer	5.6
Total volume	10

The mixture was heated at 95 °C for 5 min in a thermal cycler and subsequently cooled to RT. Before forming the RNP complex, the Cas9 enzyme was diluted to a concentration of 36 μ M by mixing the following components (see **table 4.8**).

Table 4.8: Dilution of the Cas9 enzyme

Reagents	Amount (μ l)
Alt-R Cas9 enzyme (62 μ M stock)	0.3
Resuspension Buffer R (from neon system Kit)	0.2
Total volume	0.5

For the final formation of the RNP complex, the crRNA:tracrRNA duplex was combined with the diluted Alt-R Cas9 enzyme (36 μM) for each well undergoing electroporation (see **table 4.9**). The components were gently pipetted up and down and the mixture was incubated at RT for 15 min.

Table 4.9: Formation of the RNP complex

Reagents	Amount (μl)
crRNA:TracrRNA duplex	0.5 (22 pmol)
Diluted Alt-R Cas9 enzyme (36 μM)	0.5 (18 pmol)
Total volume	1

To calibrate the system, 10 μl Resuspension Buffer R were pipetted into the Neon Pipette station, which was subsequently set up by filling the Neon Tube with 3 ml Electrolytic Buffer and inserting the tube into the station. To create a stock solution, the Alt-R Cas9 Electroporation Enhancer was resuspended in IDTE Buffer to a final concentration of 100 μM . For each set of experiments, the stock solution was diluted to a 10.8 μM working solution of which 2 μl were needed for each well undergoing electroporation. Furtherly, the culture plates receiving the cells after electroporation were prepared. The necessary wells were filled with 1 ml culture medium (RPMI, 10 % FBS). The plates were stored in a tissue culture incubator (37 $^{\circ}\text{C}$, 5 % CO_2). Before counting the cells in the suspension culture, the cells were pipetted up and down to dissociate cell clumps. 2×10^5 cells were used for each well. The required number of cells was centrifuged at 300 x g for 8 min at RT. After the supernatant was removed, cells were washed in 5 ml of 1X PBS and then centrifuged again at 300 x g for 8 min at RT. Cells were resuspended in 9 μl of Resuspension Buffer R per electroporation.

For each electroporation, the following reagents were pipetted into a 200 μl tube (see **table 4.10**).

Table 4.10: Electroporation suspension composition

Reagents	Amount (µl)
RNP complex	1
Cell suspension	9
10.8 µM Alt-R Cas9 Electroporation Enhancer	2
Total volume	12

The Neon tip was inserted into the Neon pipette and 10 µl of the mixture above were pipetted into the Neon tip avoiding air bubbles. The Neon pipette and tip were inserted into the pipette Station. For electroporation, the Neon Transfection system was used according to the optimized parameters, which were predetermined via the optimization protocol (see **table 8.1a/b**). Electroporation settings were as following:

Pulse Voltage: 1600, Pulse Width: 20, Pulse Nr.: 1

After electroporation, the cells were transferred into the wells containing 1 ml of prewarmed culture medium (RPMI, 10 % FBS), followed by a slow and careful resuspension. The electroporated cells were incubated for 24-72 h.

4.2.5.3. Fluorescent Cell Analysis

4.2.5.3.1. Fluorescence Activated Cell Sorting

FACS analysis is performed by hydrodynamically focusing the cells of a single cell suspension past a focused laser beam of a suitable wavelength. When the electrons of the fluorescent dye are excited precisely by the monochromatic laser beam, they are raised to a higher energy level and when the cells pass the laser beam in single file, they emit a light scatter. The emitted photon concentration is registered by a photodetector (Sack et al., 2006). To prepare the transfected cells for the fluorescence activated cell sorting system, 500 µl of cells were pipetted into 5 ml glass flacons and washed with 4 ml of FACS Buffer twice and centrifuged at 1,200 rpm for 5 min at 4 °C. The supernatant was discarded and the pellet resuspended in 400 µl FACS Buffer and carefully vortexed. FACS analysis with the FACSymphony A5 and LSRFortessa

(Becton Dickinson, Heidelberg, Germany) was carried out by the working group of Prof. Dr. med. Matthias Edinger (Department of Internal Medicine III, University Hospital Regensburg).

4.2.5.3.2. Fluorescence Microscopy

For the fluorescence microscopy, 500 µl cell suspension were placed in a 24-well plate. The fluorescence intensity was imaged by using the Fluorescence cell Imager Zoe (Bio-Rad, Munich, Germany).

4.2.5.4. Amplification of Genomic DNA and Mutation Detection

4.2.5.4.1. DNA-Isolation

For DNA-Isolation, incubated cells were treated with the DNeasy Blood and Tissue Kit (Qiagen, Hilden, Germany). The experiments were carried out according to the instructions provided by the manufacturer, except that the DNA was eluted in 25 µl AE Buffer. The concentration was measured on the Qubit 2.0 Fluorometer (Thermo Fisher Scientific, Waltham, USA).

4.2.5.4.2. Amplification using Polymerase Chain Reaction

The Polymerase Chain Reaction (PCR) was carried out using the KAPA HiFi HotStart ReadyMix (Roche, Mannheim, Germany; see **table 4.11**).

Table 4.11: PCR Setup

Reagents	Amount
DNA (10 ng)	10 ng
Forward Primer (10 µM)	2.5 µl
Reverse Primer (10 µM)	2.5 µl
KAPA HIFI HotStart ReadyMix (2X)	25 µl
H ₂ O	Ad 50 µl

The PCR was run with the following cycling conditions listed in **table 4.12**.

Table 4.12: PCR cycling conditions

Step	Temperature (°C)	Time (min:sec)	Cycles
Denature	95	5:00	1
Denature	98	0:20	30
Anneal	67	0:15	
Extend	72	0:30	
Extend	72	2:00	1

4.2.5.4.3. DNA Cleanup

To purify the reaction outcome, DNA Cleanup was carried out with Monarch PCR & DNA Cleanup Kit (NEB, Frankfurt, Germany). Therefore, 50 µl of PCR product were diluted with 250 µl of DNA Cleanup Binding Buffer (scale up as needed) by pipetting up and down. The column was inserted into the collection tube and samples were loaded onto the column. Both were spun at 11,000 rpm for 1 min at RT and the flow-through was discarded. The column was reinserted into the collection tube and washed with 200 µl of DNA Wash Buffer and spun for 1 min. After repeating the last step, the column was transferred to a 1.5 ml microfuge tube. 15 µl of DNA-EB were added to the center of the matrix. After waiting for 1 min, the DNA was eluted by spinning again at 13,000 rpm for 1 min. The concentration was measured on the Qubit 2.0 Fluorometer (Thermo Fisher Scientific, Waltham, USA). For verification of DNA fragment sizes, a 1 % Agarose Gel Electrophoresis (see **section 4.2.2.4.4**) was carried out using 200 ng of DNA.

4.2.5.4.4. Formation of Heteroduplexes for T7 Endonuclease digestion

T7 Endonuclease assay (T7EI) represents a microbiological method to determine genome targeting efficiency by detecting DNA mismatches in CRISPR/Cas9-treated cells (Mashal et al; 1995). For the T7EI mismatch endonuclease assay, Alt-R Genome Editing Detection Kit (IDT, Coralville, USA) was used. Before T7EI was executed,

heteroduplexes were formed. For each sample, the following components in **table 4.13** were added to the PCR DNA.

Table 4.13: Formation of heteroduplexes for T7EI

Reagents	Amount
PCR DNA	200 ng
T7EI reaction Buffer	2 µl
Nuclease free water	Ad 18 µl

The reaction was heated and cooled in a thermal cycler with the parameters demonstrated in **table 4.14**.

Table 4.14: Thermal Cycler Conditions for T7EI

Step	Temperature	Time
Denature	95 °C	10 min
Ramp 1	95-85 °C	Ramp rate -0.1 °C/sec
Ramp 2	85-25 °C	Ramp rate -0.1 °C/sec

For T7 Endonuclease digestion, the following substances (see **table 4.15**) were incubated together for 60 min at 37 °C.

Table 4.15: T7 Endonuclease digestion setup

Reagents	Amount (µl)
PCR Heteroduplexes	18
T7 Endonuclease I (1U/µl)	1
Total volume	19

After incubation, the products were measured on Agilent TapeStation (Böblingen, Germany), using the HighSensitivity D1000HS setting. The percentage of genetically modified DNA was calculated using the formula below with c being the calibrated concentration (Gushin et al., 2010).

$$\text{Gene Modification [\%]} = 100 \times \left(1 - \left(1 - \frac{c_{\text{cleaved fragment}}}{c_{\text{uncleaved fragment}} + c_{\text{cleaved fragment}}} \right)^2 \right)^{\frac{1}{2}}$$

4.3. Protein Biochemical Methods

4.3.1. Preparation of Whole Cell Lysates

For each time point, 1.5×10^5 RNP complex transfected cells were harvested via centrifugation. After washing the cells with PBS, the supernatant was removed with a pipette and the cell pellet was resuspended in 15 μ l 2X SDS. They were immediately stored at -20 °C until further use. For subsequent Sodium Dodecyl Sulfate polyacrylamide gel electrophoresis (SDS-PAGE), the samples were heated for 10 min at 95 °C in a heating block and vortexed after incubation.

4.3.2. Sodium Dodecyl Sulfate Polyacrylamide Gel Electrophoresis

To allow protein separation by mass, samples were sorted by SDS-Page. Due to its higher resolution, a discontinuous gel system was used. The gel system consisted of different separating and stacking gel layers that vary in acrylamide concentration and pH value. One day before electrophoresis, the gels were produced starting with the 10 % separating gel. The gels were covered with isopropanol until completely polymerized. When the gels were fully solidified, isopropanol was removed and the 5 % stacking gel was poured on top of the 10 % stacking gel, immediately inserting a comb. The gels were kept moist overnight at 4 °C.

On the day of SDS-PAGE, the gels were mounted into an electrophoresis tank filled with 1X Laemmli buffer. The samples were loaded into the slots and the gel was run at 80 V until proteins entirely reached the surface of the stacking gel. For protein separation, the gel was run at 120 V for 1-2 h. By using the Precision Plus Protein Kaleidoscope (Bio-Rad) as a molecular weight marker, the proteins were analyzed according to their size.

4.3.3. Western Blot Analysis and Immunostaining

After separation via discontinuous SDS-Page, proteins were blotted onto a PVDF membrane (Immobilon-P, Millipore) electrophoretically using a three-buffer semi-dry transfer system. After the transfer was completed, proteins were visualized via specific

primary antibodies and horseradish peroxidase (HRP) secondary antibodies for colorimetric detection and chemiluminescent HRP substrates. PVDF membrane and filter papers were cut to the size of the gel and moistened with isopropanol and a suitable buffer. The WB setup is shown in **figure 4.1**.

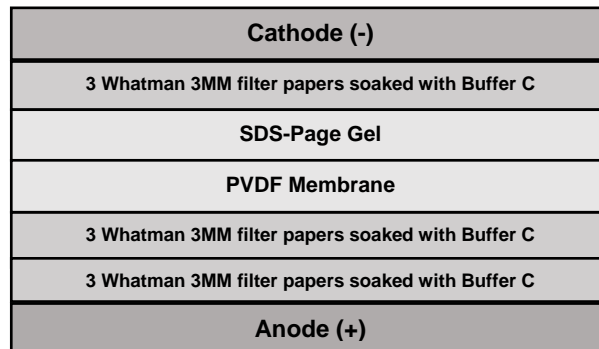


Figure 4.1: WB setup

The SDS-PAGE gel was put on top of the PVDF membrane, overlaid with three filter papers and covered with Buffer C. The cathode was placed on top of the stack. The protein transfer was run at 11 V for 60 min. Prestained bands of the protein ladder on the blotted membrane were identified and marked. The blot was washed once in H₂O with mild agitation (50–60 rpm) for about 2-3 min before blocking it with 3 % nonfat dry milk in 1X TBS (pH 8.0) for 30 min at RT. After removing the blocking agent, the blot was washed again for 10 min with TBS. Primary antibodies were added and incubation at RT for at least 60 min followed. Anti-BRG1 was used as primary antibody (diluted 1:1,000) and anti-Actin (diluted 1:2,000) served as loading control for the whole cell lysates (WCLs). Antibodies were diluted in 1X TBS containing 3 % milk. The membranes were washed again for 10 min with 1X TBS before incubation with the corresponding secondary antibody followed for at least 30 min at RT. After removing the primary antibody solution, the blot was washed again for 10 min with TBS and the HRP-coupled secondary antibody was added. The blot was again incubated with shaking for 30 min at RT. Within 20 min, eight washing steps with TBS (with Tween 20) were carried out.

To visualize the bound antibodies, the ECL Prime Western Blotting System (Sigma-Aldrich, Taufkirchen, Germany) was used. Developing was carried out with the Fusion Pulse Imaging System from Vilber Lourmat (Eberhardzell, Germany). To re-

blot the same membrane for further protein detection, the blot was washed once with 1X TBS and incubated for 15 min at RT with the 1X ReBlot Solution. The stripped blot was washed and again blocked and immunostained as described above. ImageJ was used for protein expression evaluation.

5. Results

5.1. Expression of Fluorescent Fusion Proteins in CTV-1 Cells

To visualize the interaction and to track the spatial and temporal distribution of the target proteins PU.1 and BRG1, two different FFPs were designed. To generate a color difference between the two proteins, a scarlet red and a neon green colored construct were created. To enable CTV-1 cells to express the FP, the genetic sequence of TF PU.1 was fused to the sequence of the FP. The DNA of the finished FP was subsequently cloned into vector pEF6/V5-His Topo (see **figure 5.1a/b**). The plasmid DNA was available from previous experiments, all other gBlock Gene Fragments were ordered at IDT (Coralville, USA). The respective gene sequences are listed in **section 3.8**.

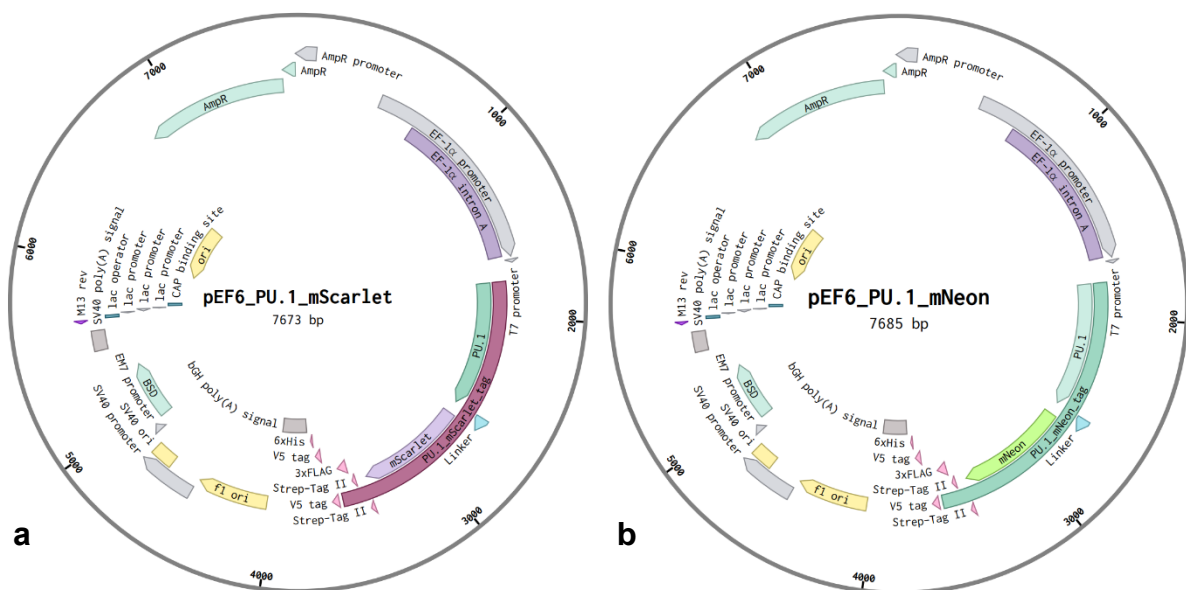


Figure 5.1a/b: pEF6/V5-His Topo vectors comprising PU.1-mScarlet and PU.1-mNeon

The figure displays the pEF6 plasmids, including the FFP coding DNA inserts. Image **a** represents the vector comprising PU.1-mScarlet, measuring 7673 bp. Image **b** shows the identical vector including the PU.1-mNeon tag with a size of 7685 bp. The plasmid displays were created with the online platform benchling.

The vector pEF6/V5-His Topo was linearized via restriction endonuclease digestion and loaded onto a 1 % agarose gel. DNA purification was carried out using Gel Extraction and the gBlocks were cloned into *DH10B* via Gibson Assembly. For permanent storage, bacterial cultures were stored in 20 % glycerol and placed in cryotubes at -80 °C. After plasmid isolation from *E. coli*, cloning success was verified by 1 % Agarose gel electrophoresis and Sanger sequencing. Subsequently, DNA was linearized using restriction endonuclease digestion. Nucleic acid was purified via Phenol/Chloroform extraction and Ethanol precipitation, before *in vitro* transcription was carried out. Plasmids were transcribed into 5`-3` polyadenylated, capped mRNA, which was furtherly used for transfection into CTV-1 cells.

5.1.1. Efficiency of Self-designed Constructs in Comparison to GFP

To put the expression efficiency of the self-designed constructs into perspective and to verify successful transfection, extra cells were transfected with *in vitro* transcribed GFP (green fluorescent protein)-mRNA. As an additional control, further cells were mock transfected with the same parameters but without mRNA. For each time point and sample, 1×10^6 cells were electroporated. After transfection, cells were incubated in RPMI medium (1 ml per 1×10^6 cells) and harvested at different time points (2 h, 4 h, 6 h, 8 h, 24 h). To generate an objective quantification of the expression efficiency, cells were analyzed using FACS analysis, which was carried out by the working group of Prof. Dr. med. Matthias Edinger (Department of Internal Medicine III, University Hospital Regensburg). The FACS plots shown in **figure 5.2a/b/c** illustrate the expression efficiency of the FP over time. As expected, mock transfected cells show no expression of the fluorescent protein, whereas GFP-mRNA transfected cells show a transfection efficiency of almost 100 %, which proves a successful transfection process. No fluorescent expression was detected in scarlet-mRNA transfected CTV-1 cells, which leads to the conclusion that the fluorescent protein is not expressed. The transfection efficiency in neon-mRNA transfected cells was around 40 % after 4 h, then gradually decreasing to 25 % after 8 h and to 0 % after 24 h. Though neon-mRNA was expressed, GFP-mRNA was expressed on a higher level and more constant over a longer time period. For this reason, GFP as fluorescent tag was preferred over the self-designed fluorescent constructs for further experiments.

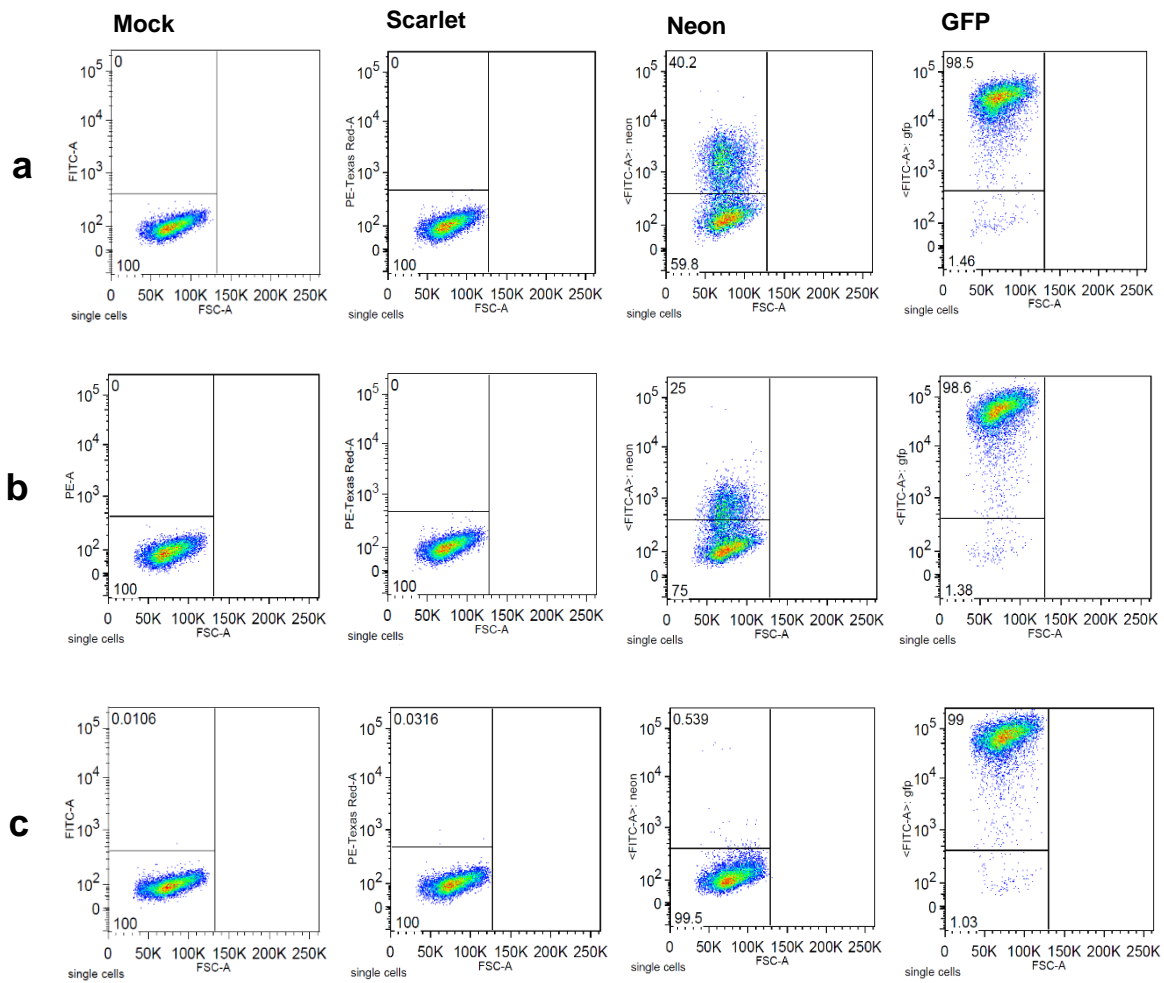


Figure 5.2a/b/c: FACS Analysis of transfected CTV-1 cells

Depicted are the FACS plots of mock, Scarlet-mRNA, Neon-mRNA and GFP-mRNA transfected cells. The figure illustrates the expression of the FFP at three different time points. The first series of plots (a) shows cells harvested after 4 h, the second series (b) after 8 h and the third series (c) after 24 h incubation. The percentage of cells expressing the FP is indicated in the upper left corner. In the mock and Scarlet-mRNA transfected cells, no fluorescence could be detected. The Neon-mRNA cells expressed the FP to a certain extent, with a maximum of around 40 % expression after 4 h. GFP-mRNA transfected cells showed almost 100 % expression of the green FP throughout all time points. FACS analysis was carried out by the working group of Prof. Dr. med. Matthias Edinger (Department of Internal Medicine III, University Hospital Regensburg).

5.1.2. Efficiency of different Linker Peptides - Flexible Linker vs. 2A-Peptide

The successful construction of a recombinant FP also requires the selection of a sufficient linker. To analyze linker efficiencies, eGFP (enhanced green fluorescent protein)-mRNA was fused to PU.1 using two different linker variants: the P2A and the

FL polypeptide, illustrated in **figure 5.3a/b** (for amino acid sequences see **section 3.8**). FLs are – as the name suggests – very flexible due to their small amino acids, allowing a certain extent of mobility of the conjoined proteins. They stay bound to their adjacent proteins and are useful linkers, when movement or interaction between the proteins is desired (Chen et al., 2013). P2A linkers, on the other hand, are small oligopeptides, which mediate *in vivo* cleavage within their sequence next to their downstream peptide, consequently resulting in two cleaved proteins (Kim et al., 2011). This leads to a simultaneous co-expression of PU.1 and eGFP. The GSG (Gly-Ser-Gly)-linker N-terminally upstream of the 2A-peptide enhances its effectiveness. The Kozak sequence (Kozak seq) is recognized by ribosomes and is important for the start of translation during protein biosynthesis. Both additional protein tags, Strep-tag II (ST II) and the 3x Flag-tag are specific polypeptide tags, that serve as artificial antigens and allow high-affinity chromatography purification and detection.

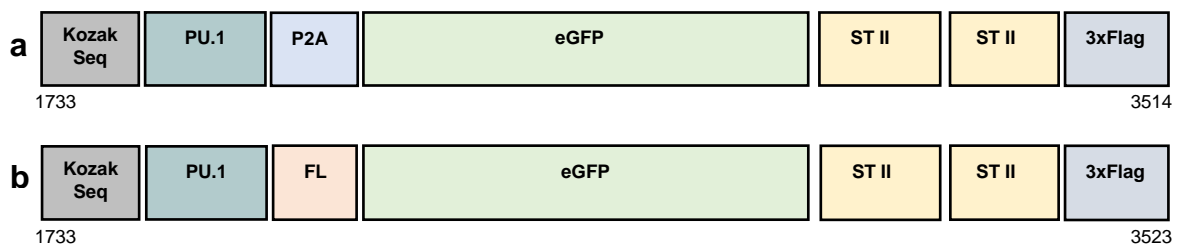


Figure 5.3a/b: Structures of fluorescent PU.1-eGFP-linker constructs

The eGFP-mRNA is fused to the P2A-sequence (a) and to the FL-sequence (b). Both constructs comprise a Kozak Sequence, two Strep-tag II and a 3x Flag-tag. The number of bp is indicated below.

The cloning and verification process was identical to the description above in **section 5.1.1**. For each sample and time point, 2×10^6 CTV-1 cells were electroporated with the electroporation parameters seen in **section 4.2.5.1**. After transfection, 1×10^6 cells/ml were incubated in RPMI medium and harvested after 4 h and 24 h. Further analyses were carried out via FACS and the Zoe Fluorescence Cell Imager. Additional CTV-1 cells were mock transfected to check for possible cellular impact due to transfection reagent exposure.

5.1.2.1. FACS Analysis of GFP transfected CTV-1 Cells

The FACS plots in **figure 5.4** visualize the percentage of GFP-positive (gfp+) cells. The GFP expression in mock transfected cells is at both time points, as expected, close to 0 %. Approximately half of all cells transfected with the P2A-eGFP construct express GFP after 4 h (**a**) and after 24 h (**b**) about 37 % of the cells were still GFP-positive. The GFP expression of cells containing the FL-eGFP construct is at 92 % after 4 h (**a**) but rapidly decreases to only 1 % after 24 h of incubation (**b**).

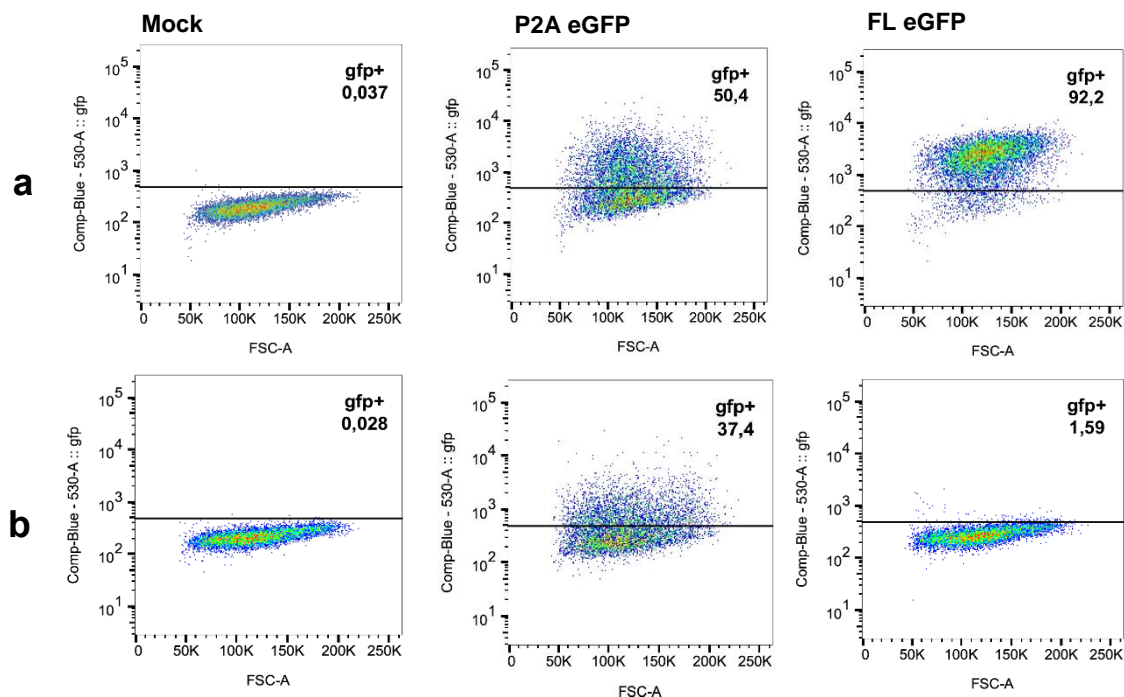


Figure 5.4: FACS analysis of different linker variants in GFP transfected CTV-1 cells

The depicted FACS plots represent the percentage of CTV-1 cells that express the green FP (GFP). The percentage is indicated in the upper right corner. Dots above the horizontal line represent GFP-positive cells. The first series of blots (**a**) shows cells harvested after 4 h of incubation, whereas the second series (**b**) depicts blots after 24 h of incubation. FACS analysis was carried out by the working group of Prof. Dr. med. Matthias Edinger (Department of Internal Medicine III, University Hospital Regensburg).

5.1.2.2. Fluorescent Cell Imaging

To further illustrate GFP expression, 1×10^6 transfected cells were harvested after 4 h of incubation and examined under the Zoe Fluorescence Cell Imager. As expected,

figure 5.5 shows that mock transfected cells do not appear fluorescent, whereas the FL-eGFP and the P2A-eGFP transfected cells are fluorescent post transfection. Although a difference of approximately 58 % in expression efficiency between the two different linker constructs was shown in the corresponding FACS analysis, the precise graduation could not be detected with the Zoe Fluorescence Cell Imager. Likewise, it is not possible to localize the fluorescent protein within the cellular structures. Nevertheless, the images prove the successful transfection and that both linker constructs result in a functional FFP.

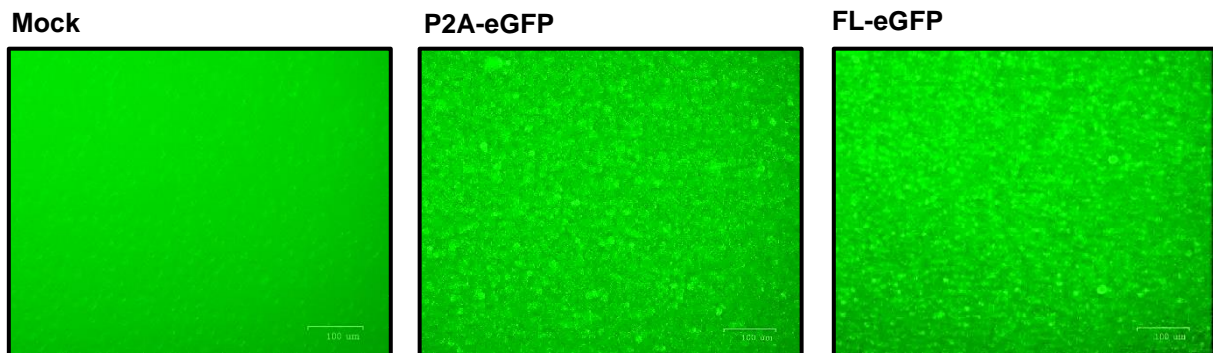


Figure 5.5: Fluorescent cell images of GFP transfected CTV-1 cells

The images illustrate eGFP transfected cells with different linker variants after 4 h of incubation. As expected, the left image proves that mock transfected cells do not emit any fluorescence. The second image depicts P2A-eGFP transfected cells and the third image shows FL-eGFP transfected cells, which both appear fluorescent under illumination in the green channel. The images were all equally optimized in contrast and sharpness. The molecular size standard is 100 μm .

5.2. Genetic Manipulation in the Gene Locus of BRG1 in CTV-1 Cells

The second part of this work aims at establishing a genetic manipulation using CRISPR/CAS9 in the gene locus of BRG1. This serves to insert an HDR template later on. To achieve optimized cell transfection conditions, an optimization protocol for CTV-1 cells was carried out.

5.2.1. Optimization of Electroporation Settings for CTV-1 Cells

The yield of the electroporation product is mainly dependent on the combination of the following three electric parameters: the electric field, pulse width and pulse number. To determine the most efficient electroporation combination for CTV-1 cells, different parameters were combined and the outcome was analyzed. The optimization protocol was adjusted from the 24-well optimization protocol for suspension cell lines for the Neon transfection system (Thermo Fisher Scientific, Waltham, USA). Therefore, CTV-1 cells were GFP transfected with 1 µg GFP-mRNA per 1 x 10⁶ cells. Prior to the following FACS analysis, the cells were stained with DAPI to obtain an overview of the fraction of living cells. After 4 h of incubation in the RPMI medium, the cells were analyzed via FACS. For the optimization parameters and results see **table 8.1a/b** in the appendix. The respective FACS plots of CTV-1 cells transfected with the best result parameters can be seen in **figure 5.6**.

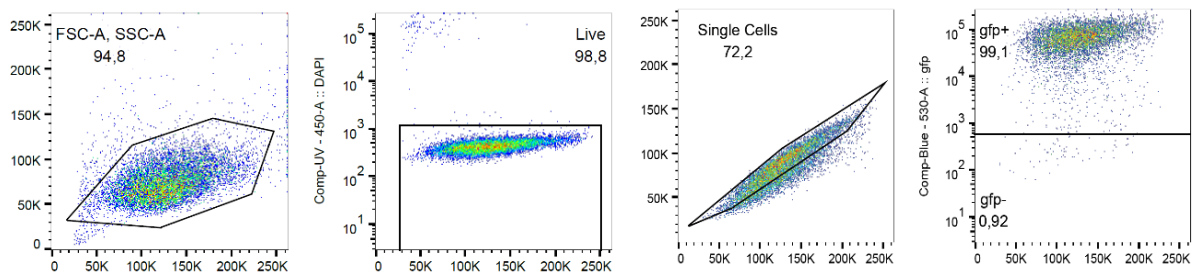


Figure 5.6: FACS plots of chosen parameters from optimization protocol

The figure shows the FACS plots of sample no. 4 with the overall best results. Cell viability (Live) is shown in the second plot. Living cells are localized within the square, whereas dead cells are localized around. The cell viability percentage was 98.8 %. Transfection efficiency (gfp+) is shown in the fourth plot. Cells localized above the horizontal line are gfp+ and therefore transfection efficient. The percentage of GFP-positive cells was 99.1 %. FACS analysis was carried out by the working group of Prof. Dr. med. Matthias Edinger (Department of Internal Medicine III, University Hospital Regensburg).

It was shown that cell transfection was successful and that CTV-1 cells are therefore suited for electroporation with the Neon transfection system. The most favorable parameters were obtained with sample 4 (*pulse voltage: 1600 V, pulse width: 20, pulse number: 1*). In addition, slight trends within the protocol were observed (see **table 8.1a/b**). Cell viability decreased with increasing pulse number, whereas GFP expression remained unchanged at a constant high level. Sample 11 was not correctly transfected and therefore represents a downward outlier in GFP expression. The best

cell viability was achieved in sample 1, which served as a control and was not transfected. Nevertheless, the difference between the cell viability of the transfected cells compared to the non-transfected cells can be neglected.

5.2.2. Determination of Genome Targeting Efficiency via T7 Endonuclease Assay

To establish genetic manipulation in the BRG1 locus, the CRISPR/Cas9 method was used. The CRISPR/Cas9 system allows site-specific genome engineering, by mediating DNA double-strand break (Jinek et al., 2012). These breaks can be later repaired with homology-directed repair (HDR)-templates and the desired mutation can be introduced via the homologous regions.

To enable later HDR-template introduction and to avoid possible influences on the protein function, the designed gRNA was located in the non-coding area, 4 bp upstream of the coding region in Exon 36 (for gRNA sequence see **section 3.8**) close to the TGA stop codon. A forward primer and a reverse primer were designed about 490 bp up- and downstream of the gRNA region. Primers were measuring 20-25 bp, as schematically illustrated in **figure 5.7**. The whole gene fragment, including primer sequences, was measuring 986 bp. A more precise representation of the DNA fragment is shown in **figure 8.1** in the appendix.

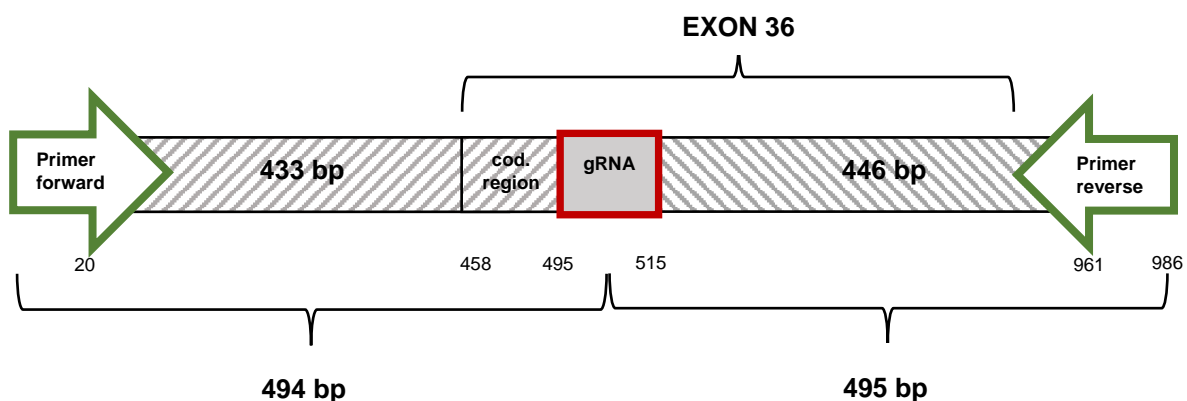


Figure 5.7: Schematic representation of the DNA fragment

This figure schematically illustrates the DNA fragment amplified by PCR. The primer sequences are located at each end of the gene fragment. The gRNA target region is located in the middle, which results in two DNA fragments of approximately equal size (~490 bp) after genetic modification.

Transfection of the RNP complex (see **section 4.2.5.2**) was carried out with the predetermined parameters from **section 5.2.1**. The cells were incubated after transfection and their DNA was isolated. The DNA was amplified using PCR (see **section 3.8** for primer sequences). The genome targeting efficiency was measured via T7EI, by recognizing DNA mismatches in CRISPR/Cas9-treated cells. T7 Endonuclease I detects mismatched DNA and catalyzes DNA cleavage at the respective site (Mashal et al., 1995; Sentmanat et al., 2018). For the T7EI, Heteroduplexes were formed and the results were measured on the Agilent TapeStation (see **figure 5.8**).

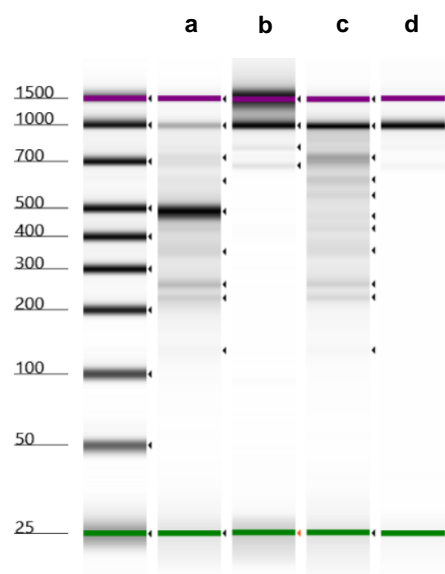


Figure 5.8: T7EI results

*The figure illustrates the genome targeting efficiency measured on the Agilent TapeStation. The D1000 Electronic ladder for TapeStation was used for molecular sizing. Sample **a** shows DNA fragments from RNP complex transfected cells, which were subsequently digested with the T7 Endonuclease. Sample lane **b** indicates DNA fragments from RNP complex transfected cells, which did not undergo T7 Endonuclease digestion. Sample **c** shows DNA fragments from mock transfected and T7 Endonuclease digested cells. DNA fragments from undigested, mock transfected cells are represented in lane **d**.*

Figure 5.8 depicts the results after T7EI. The results indicate the successful establishment of the genetic manipulation at the desired target site. As expected, sample lane **a** shows DNA-fragments from RNP complex transfected cells post T7 Endonuclease digestion. A clear band at ~490 bp can be observed, compared to the undigested samples in lane **b**. The bands from digested (**c**) and undigested (**d**) mock transfected cells are also depicted and support the above-mentioned thesis, since the peak at ~490 bp is not observed. As illustrated in **figure 5.9a/b**, the band in

sample **a** also shows a newly emerged peak at the level of ~490 bp, which matches the cleaved DNA fragments' sizes. Since this peak cannot be observed in sample **b**, the bands must have appeared after T7 Endonuclease digestion. The intensity of the band at ~1000 bp, which represents the uncut DNA fragment, in sample **a** with an integrated area of 8.97 %, is about 10 times less than in sample **b** with 87.27 %. This again confirms that the newly created fragments are cut parts of the original fragment. The faint bands at the level of approximately 735 bp, 619 bp, 263 bp, 229 bp and 137 bp can also be seen in the T7 Endonuclease digested mock control, suggesting that the amplified region contains natural allelic variants, which are also detected by the T7 assay.

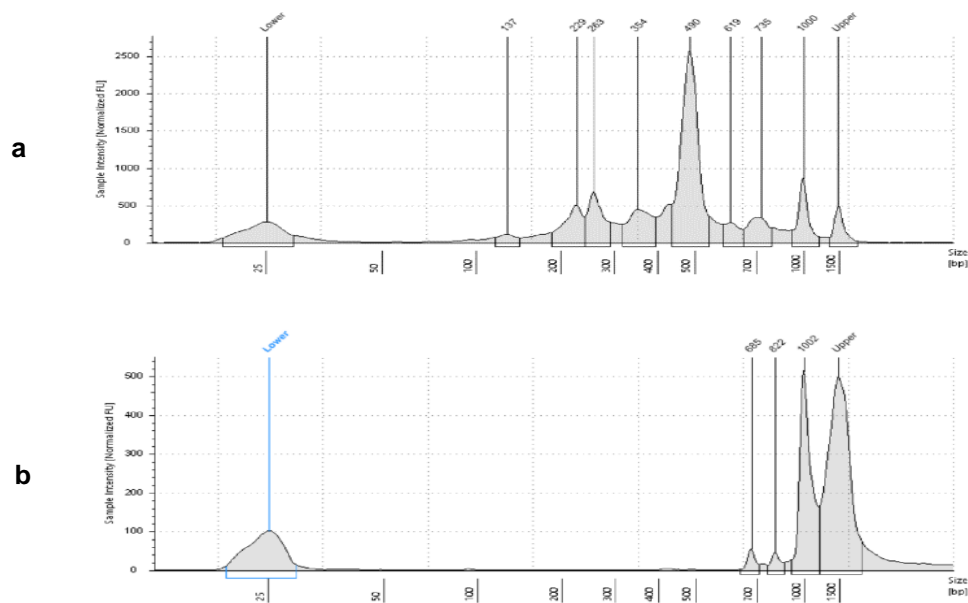


Figure 5.9a/b: Sample intensities of DNA fragments after T7EI

In this diagram, the DNA fragment size was plotted against its intensity. The diagrams show DNA fragments from RNP complex transfected cells, which underwent T7 Endonuclease digestion (**a**) or not (**b**). Visible in **a** is the newly emerged peak at ~490 bp with an integrated area of 46.07 %. Moreover, the intensity of the peak at ~1000 bp with an integrated area of 8.97 % is almost 10 times less compared to the same peak in **b** with 87.27 %.

5.2.3. Time-dependent Western Blot Analysis of transfected CTV-1 Cells

CTV-1 cells were transfected with the RNP complex and WCLs were prepared (see **section 4.2.5.2**). To verify successful BRG1 protein expression after CRISPR/Cas9-mediated genome editing, CTV-1 cells were analyzed via WB, using an

anti-BRG1 antibody (~185 kDa). Anti-actin (~42 kDa) was used as a loading control to normalize the levels of protein detected. For WB analysis, 1.5×10^5 cells were used for each sample and time point. CTV-1 cells were examined after 24 h, 48 h and 72 h of incubation. To reinsure proper BRG1 function in cells with uncut DNA, mock transfected cells were additionally analyzed as seen in **figure 5.10a/b**.

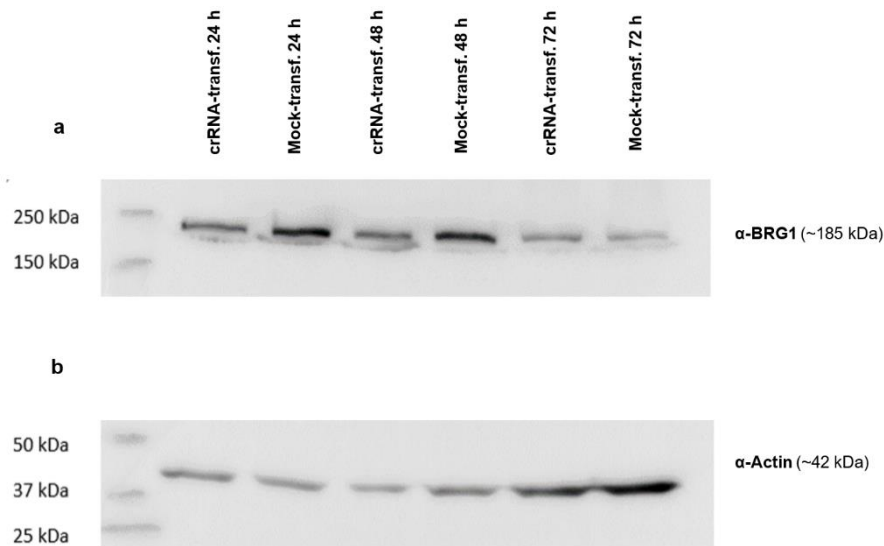


Figure 5.10a/b: WB analysis of BRG1 expression in CTV-1 cells

CTV-1 cells were transfected with the RNP complex and WCLs were prepared. The lysates were analyzed via WB after 24 h, 48 h and 72 h. The WB shows the time-dependent expression of BRG1 in the WCLs. The blots were also stained with an anti-actin antibody. Figure a depicts two bands at ~185 kDa for each time point. As depicted in figure b, α -Actin ~42 kDa served as loading control.

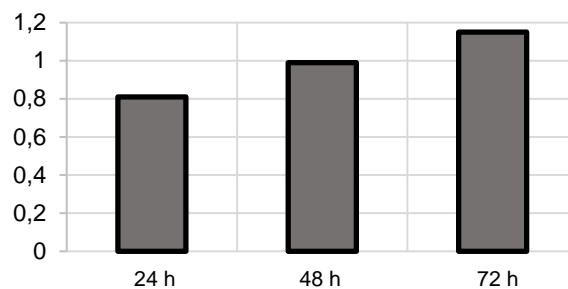


Figure 5.11: Quantification of the expression level of BRG1

The figure shows the actin-normalized BRG1 protein expression of the RNP complex transfected cells in relation to their respective mock transfected cells. The BRG1 expression percentage is plotted against the different time points. The expression levels of BRG1 in RNP complex transfected cells equal approximately 81 % after 24 h, to 99 % after 48 h and up to 115 % after 72 h. The percentages were calculated using ImageJ.

The WB image demonstrates the expression of BRG1 in WCLs at different time points after CRISPR/Cas9-mediated gene manipulation (see **figure 5.10a/b**). Notably, all samples on the blot express the BRG1 protein. The quantified level of protein expression of the RNP complex transfected cells in comparison to the mock transfected cells was calculated. After 24 h the expression level of BRG1 in RNP complex transfected cells amounts to approximately 81 %, after 48 h to 99 % up to 115 % after 72 h (see **figure 5.11**) in relation to mock transfected cells. This proves that the cut in BRG1 was made at the intended target site in the non-coding area and is suitable for inserting a FP for further experiments. According to the WB carried out, the function of the BRG1 protein remains unaffected.

5.2.4. Growth and Morphology of CTV-1 Cells post Transfection

In order to rule out a further growth deficit due to the transfection and gene editing process, CTV-1 cells were counted and the morphology was evaluated under the EVOS Cell Imaging System at each time point at 24 h, 48 h and 72 h (see **figures 5.12** and **5.13a/b**).

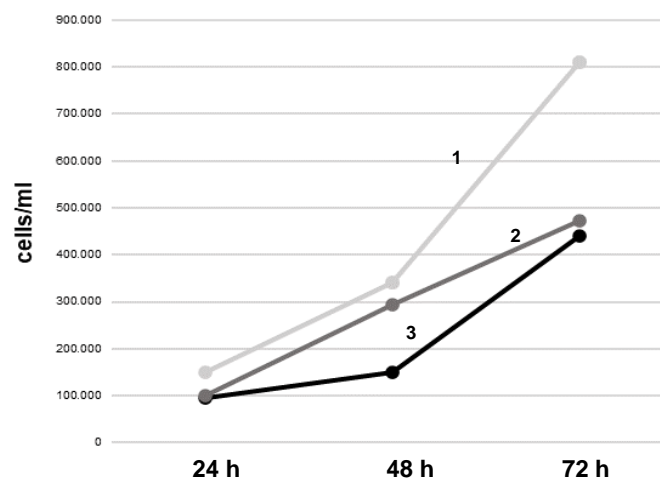


Figure 5.12: Growth of CTV-1 cells post transfection

The figure depicts the growth of CTV-1 cells after RNP complex transfection and subsequent CRISPR/Cas9-mediated gene editing. Line 1 represents cell growth of mock transfected CTV-1 cells, line 2 the average growth of CTV-1 cells in cell culture and line 3 the cell growth of RNP complex transfected CTV-1 cells.

As seen in **figure 5.12**, the average doubling time of cell culture growth of non-transfected CTV-1 was approximately 36 h. As a baseline, 1×10^5 cells were seeded. After 24 h, the cell number only slightly changed, between 0.95×10^5 cells/ml for the RNP complex transfected cells compared to 1.5×10^5 cells/ml for the mock transfected cells. After 48 h, the cell number steadily increased, with 1.5×10^5 cells/ml in the RNP complex transfected cells and 3.4×10^5 cells/ml in the mock transfected cells. On day 3, cell density was at 4.4×10^5 cells/ml in RNP complex transfected cells and 8.1×10^5 in mock transfected cells. This demonstrates good cell growth, regardless of the transfection status. However, since this was only observed over 72 h and with a limited number of cells, this is not representative and requires further investigation.

Cell morphology after 72 h was evaluated under the EVOS Cell Imaging System. This was used to assess whether the external cellular appearance has been altered by the transfection process and especially whether any differences in morphology can be observed between mock and RNP complex transfected cells (see **figure 5.13a/b**).

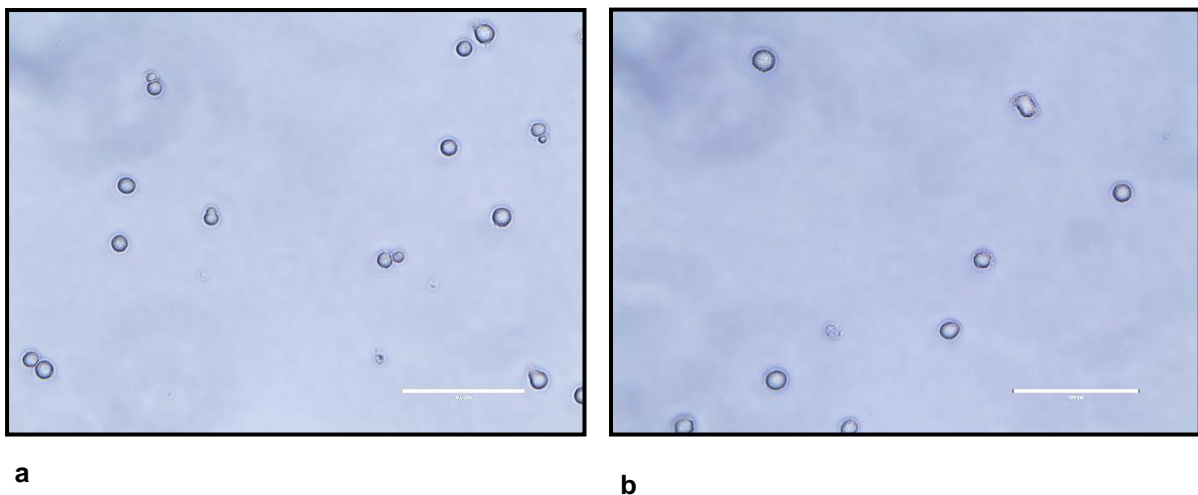


Figure 5.13a/b: Morphology of transfected CTV-1 cells

The images illustrate mock transfected CTV-1 cells (a) and RNP complex transfected cells (b). No difference in cell size and cell morphology can be detected between the two images. The scale is 100 μ m.

Shown are CTV-1 cells transfected with the RNP complex (**b**) and mock transfected (**a**) cells. Both images depict round, multiformed cells, which resemble the original external characteristics of non-transfected cells. Cells are either singly or clustered as

two in suspension. No difference in cell morphology between mock transfected and RNP complex transfected cells is seen. This leads to the conclusion, that transfecting CTV-1 cells with the RNP complex and the subsequent genetic cut with the CRISPR/Cas9-system does not affect cell culture growth, nor their outer morphology.

6. Discussion

TFs do not only have the ability to interact with DNA but can also influence other TFs and restrict their function and DNA accessibility. The manner of how TFs interact with each other and the impact it has on the biology of the participating TFs is a fundamental aspect in transcriptional regulation, but only partially understood yet. One of the larger TF-families is the ETS-family, comprising 27 ETS-genes and 11 subfamilies (Donaldson et al., 1996). The well-studied master TF PU.1, belonging to the SPI TF subfamily and encoded by the SPI1 gene, serves as a key regulator in monocytic, macrophage and B lymphocytic lineages (Klemsz et al., 1990). Although PU.1 can be categorized as pioneer TF, it was shown that PU.1 lacks the ability of binding to nucleosome-bound targets (Kadoch and Crabtree, 2015). It has been demonstrated that the myeloid TF PU.1 can interact with members of the SWI/SNF subfamily, including BRG1 (encoded by *SMARCA4*) (Minderjahn et al., 2020). The ATP-dependent chromatin remodeling complex BRG1 can change the chromatin landscape by altering the locus of nucleosomes (Tang et al., 2010).

Nevertheless, the exact mechanisms of the interaction between PU.1 and BRG1 still remain unclear. To furtherly investigate the relation between PU.1 and BRG1, model systems are needed. This thesis focuses on the design and selection of a suitable fluorescent protein-PU.1 fusion and on establishing a genetic manipulation in the gene locus of BRG1. To validate the fluorescent FPs, preliminary mRNA transfection experiments and FACS analysis were carried out. Genetic manipulation was performed using the CRISPR/Cas9 method by transfecting a self-designed gRNA as RNP complex into CTV-1 cells. Verification of successful genetic manipulation and BRG1 protein function post transfection was carried out using T7E1 and WB. This work aims at illuminating the interplay between BRG1 and PU.1 and therefore contributes to a more profound understanding of the way they interact and the impact it has on their mutual biology.

6.1. CRISPR/Cas9-mediated BRG1 Targeting

In this thesis, SWI/SNF-subunit targeting was performed using the CRISPR/Cas9 technology as genome-editing tool. Previous studies from Schick et al. also demonstrated that CRISPR/Cas9-mediated knock-ins in the endogenous locus of BRG1 represent a successful way of BRG1 targeting. By knocking the dTag into the SMARCA4 locus, the acute degradation of BAF subunits was induced. This resulted in lower SMARCA4 protein levels and alterations of transcription and chromatin accessibility (Schick et al., 2021). Recent research on BRG1 inhibition, published in the Journal of Medicinal Chemistry, introduced the BRM014 compound, an allosteric dual inhibitor and a potent tool for BRG1 inhibition, which has already shown antiproliferative effect in BRG1-mutant-lung-tumor xenograft (Papillon et al., 2018). With this new finding, further experiments were carried out with BRM014, indicating that long-term BRG1 inhibition and the resulting loss of function leads to changes in chromatin accessibility, also proving that TF binding and the resulting effects on DNA accessibility represent a dynamic process (Iurlaro et al., 2021). In contrast to the previously mentioned publications, in this thesis, no inhibition of BRG1 was intended, since the maintenance of BRG1's function is crucial to demonstrate its impact on the biology of the interacting proteins. Therefore the 20-base gRNA (see **section 3.8**) was designed 4 bp upstream of the coding region in Exon 36 complementary to the 20 bp DNA target sequence. Also, for steric reasons, it makes sense to perform the genetic manipulation in the last exon, at the end of the protein. Thus, steric hindrance in the folding process of the protein is least likely (Snapp, 2005). The DNA recognition site is next to the PAM (protospacer adjacent motif)-sequence which triggers the CAS9 enzyme, assembled with the gRNA, to implement the double-strand break (DSB) at the desired DNA target site (Jinek et al., 2012). As illustrated in **figure 5.8 and 5.9a/b**, the DNA fragments from RNP complex transfected cells, which were subsequently digested with the T7 Endonuclease, show a newly emerged peak at ~490 bp. Since the bp size corresponds to the sizes of the cleaved DNA fragments and the band cannot be observed in the other samples, it suggests that the genetic manipulation was successful. The calculated percentage of gene modification to estimate genome targeting efficiency (see **section 4.2.5.4.4** for formula), amounts to approximately 60 %. Therefore, the genetic manipulation worked very well and was carried out with

a very high genome targeting efficiency, which is not a matter of course. The proper BRG1 expression was verified via WB analysis. As illustrated in the WB images **figure 5.10a/b**, a large proportion of BRG1 protein was detected by the BRG1 antibody, leading to the conclusion that the BRG1 protein was folded correctly and consequently functioning properly. The genetic cut was successfully established by the CRISPR/Cas9 system in the targeted region, which was located downstream of the coding region. Due to this intended localization, no restriction of protein function was expected. However, to a certain extent, the Cas9 enzyme leads to off-target cleavages and unclean cuts, that deviate from the original intended site. Hence, misfolding can occur, which can lead to a not properly working protein. The incorrect functioning protein in turn cannot be detected by the respective antibody anti-BRG1, resulting in a lower BRG1 expression in the WB, to which the lower irregularity in the percentage after 24 h may be attributed to. Nevertheless, these minor irregularities can be neglected, since the correct BRG1 function could be clearly verified through WB. This leads to the conclusion, that the genetic manipulation carried out in this thesis is well suited for further HDR-mediated degron insertion, subsequently resulting in the desired DNA alteration. Consequently, the performed CRISPR/Cas9-mediated targeting represents a promising way of establishing a genetic manipulation in the gene locus of BRG1 for further DNA modification.

6.2. Selection of Fluorescent Protein-PU.1 fusion

As mentioned above, previous BRG1-inhibition experiments have already shown to influence the interaction between PU.1 and SWI/SNF chromatin remodeling complexes, but for visualizing their interaction further investigation is necessary (Minderjahn et al., 2020). In order to be able to illuminate protein interaction, genetic targeting is followed by the insertion of fluorescent reporters. This results in a functional fluorescent protein-PU.1 fusion, which helps to illuminate protein dynamic and time-dependent distribution. As fluorescent reporters, mNeon (green) and mScarlet (red) were selected. Recent publications show, that neon fluorophores are very intense and bright fluorescent proteins. They have a high quantum yield, which in some cases exceeds that of other monomeric FPs. Therefore, neon fluorophores serve as useful alternatives for protein tagging (Bindels et al., 2016; Hostettler et al., 2017). The well-

studied “gold-standard” for FPs, *in vitro* transcribed enhanced green fluorescent protein (eGFP)-mRNA was used as a control. GFP is well suited as indicator gene, since the tripeptide Ser65-Tyr66-Gly6 autocatalytically converts into a fluorophore, thus not requiring the action of further cofactors (Heim et al., 1994). Three different FPs were designed and the efficiency of the fluorescently tagged cells was examined via FACS (see **section 5.1.1**). As seen in **figure 5.2a/b/c**, no fluorescence could be detected at any time point in scarlet-mRNA, nor in mock transfected CTV-1 cells, which led to the conclusion that the scarlet-mRNA was not translated into a functioning scarlet red FFP. The efficiency in neon-mRNA transfected cells was around 40 % after 4h, then gradually decreasing to 0 % after 24 h. Though neon-mRNA was expressed, eGFP-mRNA was expressed at a higher level of almost 100 % at all time points and therefore more constant over time, indicating that the *in vitro* transcribed eGFP-PU.1 mRNA was entirely translated into a stable, functioning FP. Overall, the brightest FP with the highest fluorescence intensity and the lowest signal-to-noise ratio is to be preferred (Snapp, 2005). This suggests that eGFP-mRNA as fluorescent tag is favorable over the self-designed neon fluorescent constructs for further experiments. Previous research regarding the binding domain of PU.1, which was carried out with GFP-PU.1 FPs, also indicates its applicability for further testing (Zhong et al., 2005). To generate space between the fluorescent reporter and its host protein and to minimize the risk of possible folding interferences, two different linker variants, joining PU.1 and eGFP, were analyzed: the P2A and the FL polypeptide (see **figure 5.3a/b**). P2A is an *in vivo* cleavable linker, which is used to split a protein in two at a targeted site. FLs remain bound to their adjacent protein and - as the name suggests - allow a certain extent of movement and mobility of the connecting functional domain (Chen et al., 2013). As seen in **section 5.1.2**, the fluorescent emission of the P2A-FP lasted longer than the fluorescence of the FL-FP construct. Since the 2A-sequence inhibits the formation of a regular peptide bond during translation, the separation of the fluorescent tag from the PU.1 protein follows. This leads to a long-lasting eGFP expression since the P2A-eGFP construct alone is more stable than fused to the PU.1 protein. On the other hand, the FL construct was very efficient after 4 h but immensely decreased in efficiency after 24 h. This can be explained due to the biology of FLs. As already mentioned above, the FL stays bound to its host protein. This can lead, depending on the host protein’s stability, to a less stable FP, meaning that the FFP is only as stable as the PU.1 protein. In this case, the host protein PU.1 was less stable

than eGFP, leading to a higher eGFP expression of the P2A construct after 24 h, compared to the FL construct. Nevertheless, since the FL remains bound to PU.1 it best reflects the biology of the tagged protein. Consequently, the FL is favorable over the P2A linker for further experiments. If the use of a linker peptide due to steric hindrance reasons is necessary at all for the proper function of the FPs was not clarified in this work and requires further testing. A major disadvantage of fluorescent fusion reporters like (e)GFP is the not neglectable size (Snapp, 2005). Often discussed is also a great correlation between the folding ability of the fluorescent protein and its host protein (Waldo et al., 1999). Although it is said that fluorescent reporters fold less efficiently when attached to other proteins, it can be observed throughout all FACS plots, that the folding process of the PU.1-eGFP FP worked very well and that no steric interference can be seen. This supports the hypothesis that the fluorescent reporter does not unintentionally interfere with its host protein and that the folding process of eGFP, when attached to another well-folding protein, is not negatively affected (Sacchetti and Alberti, 1999). This thesis mainly focuses on the fluorescence of the elaborated FFPs. To furtherly test the actual protein-functionality in terms of DNA binding and chromatin distribution, the application of Chromatin Immunoprecipitation Sequencing (Chip-Seq) is recommended.

6.3. Perspectives

This thesis publishes *in vitro* model systems that enable a more precise study of the interplay of the pioneer TF PU.1 and the chromatin remodeling complex ATPase BRG1. The model systems include the design and selection of a sufficient PU.1-eGFP fusion, followed by the establishment of a genetic manipulation in the gene locus of BRG1. The validation of the self-designed FPs was performed via mRNA transfection and the different FPs were subsequently analyzed via FACS. Gene editing was carried out by CRISPR/Cas9-technology and its efficiency was measured via T7 Endonuclease assay and WB. The performed genetic manipulation serves to introduce degrons later by using CRISPR/Cas9-mediated homology-directed repair (HDR). While the final design of the degron still remains open, the FP models serve as useful guides. In addition, it is not conclusively determined yet, whether the size of the fluorescent protein may pose a steric hindrance in the subsequent folding of the

protein. According to the experiments carried out in this thesis, it seems that neither cellular function nor growth or cell morphology changes after genetic manipulation. However, the experiments were only carried out with a limited number of cells over a short period of time. To be able to clarify this conclusively and to obtain a more representative statement, further ongoing analyses are already performed. As of now, first yet to be published results with HDR-mediated degron insertions in the above-mentioned gene locus of BRG1 are promising.

7. Summary

The outcome of transcription is not solely determined by the action of a single DNA-binding transcription factor (TF), but rather by the interplay of multiple TFs and other enzymes and their combinatorial interactions with DNA (Lambert et al., 2018; Bondos and Tan, 2001; Howard and Davidson, 2004). Thus, TFs not only interact with DNA but also possess the ability to influence the biology of other enzymes. Previous work has shown that the myeloid master TF PU.1 is able to interact with individual components of chromatin remodeling complexes of the SWI/SNF family, including BRG1 (encoded by *SMARCA4*) (Minderjahn et al., 2020). The exact mechanisms of how the interaction between PU.1 and BRG1 works and the impact it plays on the biology of PU.1 is not conclusively understood yet. To perform further investigations on this topic, suitable model systems were developed in this thesis. The well-studied T-cell leukemia cell line CTV-1, which does not endogenously express PU.1, served as a model. In the first part of this thesis, for visual differentiation, a selection of fluorescent PU.1 fusion proteins (FP) was generated using cloning experiments. Validation of the proteins was carried out in advance via mRNA transfection experiments. To generate a subsequent color difference in the proteins involved, different colored fluorescent fusion proteins (FFP) were designed and compared by flow cytometry (FACS) with the already well-studied eGFP in terms of intensity and stability. This analysis revealed the superiority of GFP over the self-designed constructs. In order to generate the most stable FP and to minimize steric hindrance, further FACS analyses were used to analyze and compare different linker variants, with the FL being preferred over P2A. The second part of the work serves to establish a genetic manipulation in the gene locus of BRG1 by using the CRISPR (clustered regularly interspaced short palindromic repeats)/Cas9 system. On-target efficiency was determined via T7 Endonuclease I assay (T7EI) and BRG1 protein expression was analyzed in transfected CTV-1 cells by Western blot (WB) using anti-BRG1 antibodies. Both, the estimation of genome-modifying efficiency and BRG1 protein expression after CRISPR/Cas9-mediated genome editing, are promising. In summary, this work serves to elaborate *in vitro* models for a more detailed study of TFs and their associated proteins, thus contributing to a better understanding of the interplay between them.

8. Appendix

a

Sample	Pulse Voltage (V)	Pulse Width	Pulse No.	Cell Viability (%)	Transfection Efficiency (%)
1	0	0	0	99,2	1,73
2	1400	20	1	98,5	98,6
3	1500	20	1	98,7	98,6
4	1600	20	1	98,8	99,1
5	1700	20	1	98,7	98,0
6	1100	30	1	99,1	97,5
7	1200	30	1	98,3	98,0
8	1300	30	1	98,3	99,1
9	1400	30	1	98,4	98,9
10	1000	40	1	97,7	99,2
11	1100	40	1	98,2	79,8
12	1200	40	1	98,4	93,9
13	1100	20	2	98,5	98,2
14	1200	20	2	98,7	98,9
15	1300	20	2	98,7	98,8
16	1400	20	2	98,5	96,0
17	850	30	2	98,9	98,0
18	950	30	2	98,6	98,8
19	1050	30	2	97,8	98,2
20	1150	30	2	97,8	99,0
21	1300	10	3	97,9	98,7
22	1400	10	3	96,2	99,1
23	1500	10	3	96,1	98,9
24	1700	10	3	94,8	99,3

b

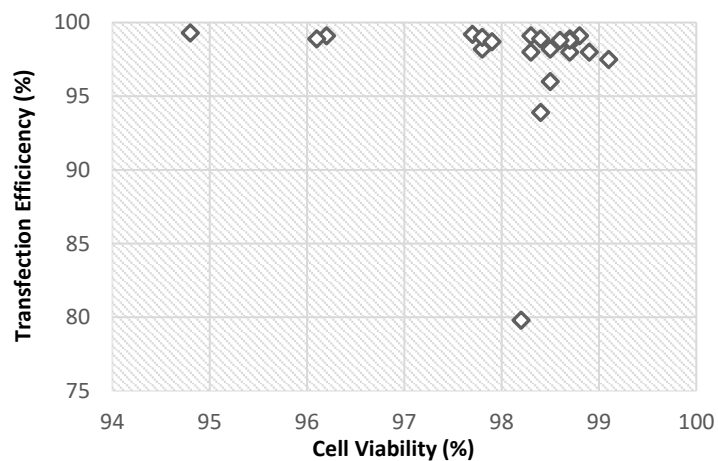
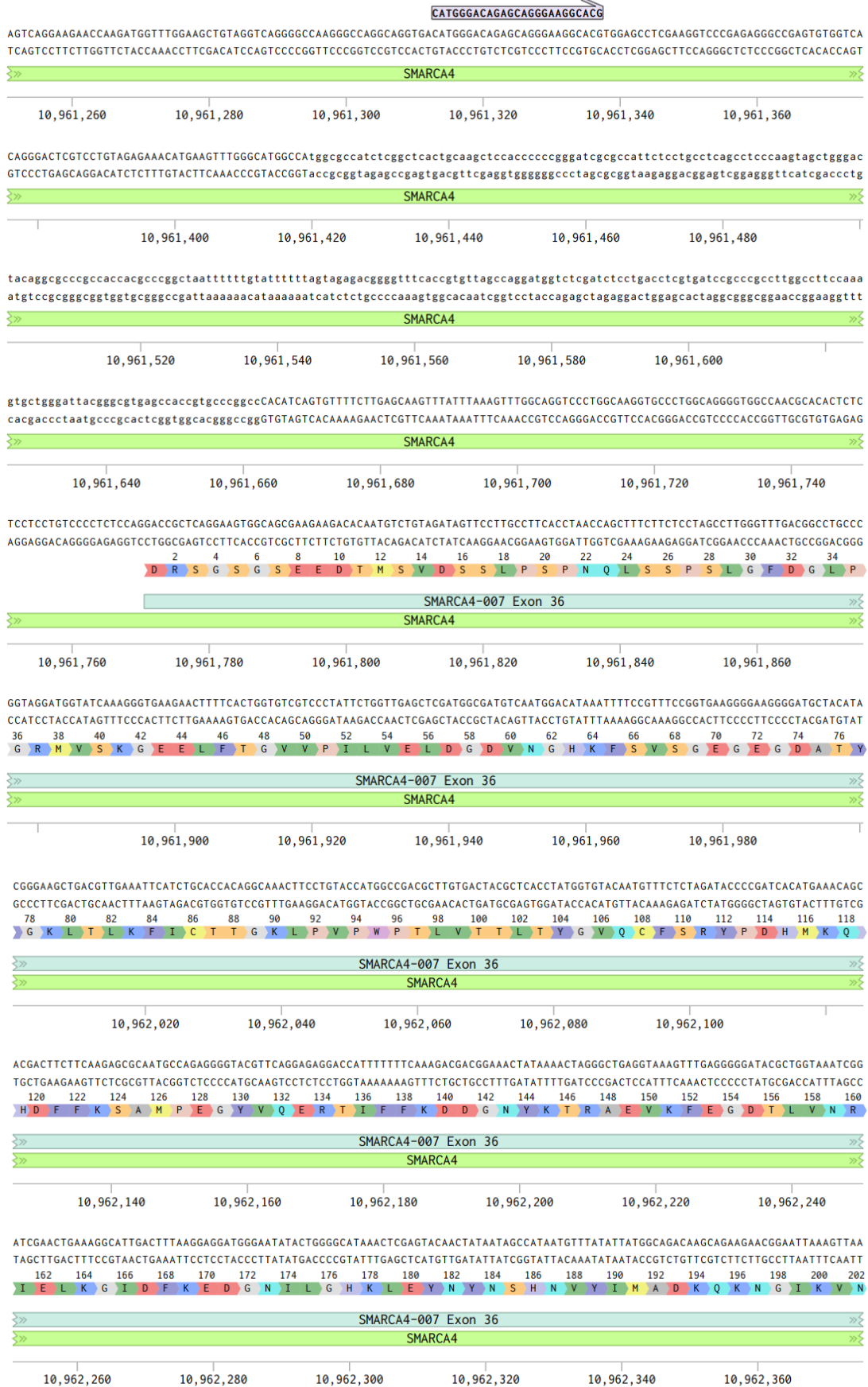


Table 8.1a/b: Optimization protocol parameters for the transfection of CTV-1-cells and results

Table **a** demonstrates the different electroporation parameters (pulse voltage, pulse width and pulse number) and the resulting transfection efficiency and cell viability. Sample 1 served as a control sample. The results of the optimization protocol are represented in figure **b**. In the diagram, the transfection efficiency is plotted against cell viability. The optimization protocol was adapted from the 24-well optimization protocol for suspension cell lines (Invitrogen, Thermo Fisher).



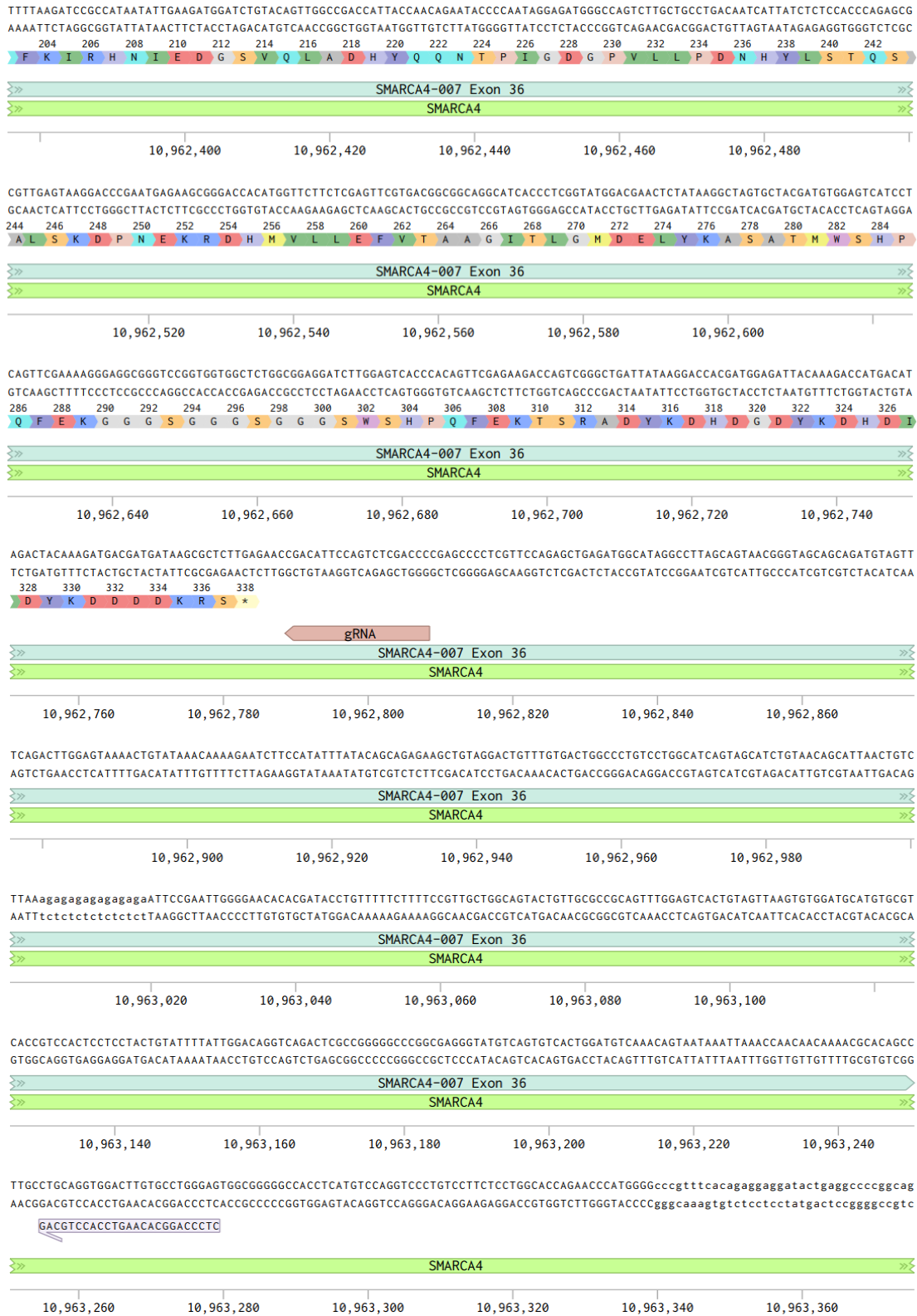


Figure 8.1: DNA Fragments for PCR amplification

The image depicts the DNA fragment amplified by PCR. The primer sequences are marked in gray and are located at the end of the gene fragment. The gRNA is marked in brown. The figure was created with benchling.

8.1. List of Figures

<i>Figure 2.1: Transcription initiation and its associated proteins</i>	10
<i>Figure 2.2: TF PU.1 and its domains</i>	13
<i>Figure 4.1: WB setup</i>	47
<i>Figure 5.1a/b: pEF6/V5-His Topo vectors comprising PU.1-mScarlet and PU.1-mNeon</i>	49
<i>Figure 5.2a/b/c: FACS Analysis of transfected CTV-1 cells</i>	51
<i>Figure 5.3a/b: Structures of fluorescent PU.1-eGFP-linker constructs</i>	52
<i>Figure 5.4: FACS analysis of different linker variants in GFP transfected CTV-1 cells</i>	53
<i>Figure 5.5: Fluorescent cell images of GFP transfected CTV-1 cells</i>	54
<i>Figure 5.6: FACS plots of chosen parameters from optimization protocol</i>	55
<i>Figure 5.7: Schematic representation of the DNA fragment</i>	56
<i>Figure 5.8: T7EI results</i>	57
<i>Figure 5.9a/b: Sample intensities of DNA fragments after T7EI</i>	58
<i>Figure 8.1: DNA Fragments for PCR amplification</i>	73

8.2. List of Tables

<i>Table 2.1: Selection of SWI/SNF subunits in mammals</i>	16
<i>Table 4.1: Linearization of the vector</i>	32
<i>Table 4.2: Gibson Assembly reaction setup</i>	34
<i>Table 4.3: Restriction enzyme digestion</i>	35
<i>Table 4.4: In vitro mRNA synthesis reaction setup</i>	37
<i>Table 4.5: Poly(A)-Tailing reaction setup</i>	38
<i>Table 4.6: Gene Pulser Xcell</i>	39
<i>Table 4.7: Formation of the crRNA:tracrRNA Duplex</i>	40
<i>Table 4.8: Dilution of the Cas9 enzyme</i>	40
<i>Table 4.9: Formation of the RNP complex</i>	41
<i>Table 4.10: Electroporation suspension composition</i>	42
<i>Table 4.11: PCR Setup</i>	43
<i>Table 4.12: PCR cycling conditions</i>	44
<i>Table 4.13: Formation of heteroduplexes for T7EI</i>	45
<i>Table 4.14: Thermal Cycler Conditions for T7EI</i>	45
<i>Table 4.15: T7 Endonuclease digestion setup</i>	45
<i>Table 8.1a/b: Optimization protocol parameters for the transfection of CTV-1-cells and results</i>	71

9. Abbreviations

ATP	adenosine triphosphate
ATPase	ATP triphosphatase
bp	base pair(s)
BRG1	brahma-related gene 1
ChIP	chromatin immunoprecipitation
CRISPR	clustered regularly interspaced short palindromic repeats
DAPI	4',6-Diamidino-2-phenylindol
DNA	deoxyribonucleic acid
DNase	deoxyribonuclease
E. coli	Escherichia coli
EB	Elution Buffer
EDTA	ethylenediaminetetraacetic acid
eGFP	enhanced green fluorescent protein
EtOH	ethanol
FACS	fluorescence-activated cell sorting
FCS	fetal calf serum
FFP	fluorescent fusion protein
FL	flexible linker
FP	fusion protein
GFP	green fluorescent protein
GTR	general transcription factor
h	hour
HDR	homology-directed repair

min	minute
mRNA	messenger ribonucleic acid
P2A	2A-Peptide
PBS	phosphate buffered saline
PCR	polymerase chain reaction
PEST	sequence rich in proline, glutamic acid, serine and threonine
PTM	posttranslational modification
rpm	rounds per minute
RT	room temperature
RTF	regulatory transcription factors
RNP	Ribonucleoprotein
SDS-PAGE	sodium dodecyl sulfate polyacrylamide gel electrophoresis
sec	seconds
Seq	sequence or sequencing
T7EI	T7 Endonuclease I assay
TAD	transactivating domain
TBS	tris buffered saline
TEMED	N,N,N',N'-Tetramethylethylenediamine
TF	transcription factor
U	units
V	volt
vs.	versus
WB	Western Blot

10. References

- Alver, B. H., Kim, K. H., Lu, P., Wang, X., Manchester, H.E., Wang, W., Haswell, J.R., Park, P. J. & Roberts C. W. M. (2017). The SWI/SNF chromatin remodelling complex is required for maintenance of lineage specific enhancers. *Nature Communications Vol. 8*, Article number: 14648. doi:10.1038/ncomms14648
- Bartel, F. O., Higuchi, T. & Spyropoulos, D. D. (2000). Mouse models in the study of the Ets family of transcription factors. *Oncogene Vol. 19(55)*, pp. 6443–6454. doi:10.1038/sj.onc.1204038
- Bell, O., Tiwari, V. K., Thomä, N. H. & Schübeler, D. D. (2011). Determinants and dynamics of genome accessibility. *Nature Reviews Genetics Vol. 12(8)*, pp. 554-564. doi:10.1038/nrg3017
- Bindels, D. S., Haarbosch, L., van Weeren, L., Postma, M., Wiese, K. E., Mastop, M., Aumonier, S., Gotthard, G., Royant, A., Hink, M. A. & Gadella, T. W. J. (2016). mScarlet: a bright monomeric red fluorescent protein for cellular imaging. *Nature Methods Vol. 14(1)*, pp. 53-56. doi:10.1038/nmeth.4047
- Bondos, S. E. & Tan, X. X. (2001). Combinatorial transcriptional regulation: the interaction of transcription factors and cell signaling molecules with homeodomain proteins in Drosophila development. *Critical reviews in eukaryotic gene expression Vol. 11(1-3)*, pp. 145-171. doi:10.1615/CritRevEukarGeneExpr.v11.i1-3.80
- Burda, P., Laslo, P. & Stopka, T. (2010). The role of PU.1 and GATA-1 transcription factors during normal and leukemogenic hematopoiesis. *Leukemia Vol. 24(7)*, pp. 1249–1257. doi:10.1038/leu.2010.104
- Buselmaier, W. (2003). *Biologie für Mediziner*. Berlin, Heidelberg: Springer-Verlag.
- Cairns, B. R., Kim, Y. J., Sayre, M. H., Laurent, B. C. & Kornberg, R. D. (1994). A multisubunit complex containing the SWI1/ADR6, SWI2/SNF2, SWI3, SNF5, and SNF6 gene products isolated from yeast. *Proceedings of the National Academy of Sciences of the United States of America (PNAS) Vol. 91(5)*, pp. 1950-1954. doi:10.1073/pnas.91.5.1950
- Carroll, S. B. (2008). Evo-Devo and an Expanding Evolutionary Synthesis: A Genetic Theory of Morphological Evolution. *Cell Vol. 134(1)*, pp. 25-36. doi:10.1016/j.cell.2008.06.030
- Chen, X., Zaro, J. L. & Shen, W. C. (2013). Fusion protein linkers: property, design and functionality. *Advanced Drug Delivery Reviews Vol. 65(10)*, pp. 1357-1369. doi:10.1016/j.addr.2012.09.039
- Choukrallah, M. A. & Matthias, P. (2014). The Interplay between Chromatin and Transcription Factor Networks during B Cell Development: Who Pulls the

- Trigger First? *Frontiers in Immunology* Vol. 5, p. 156.
doi:10.3389/fimmu.2014.00156
- Clapier, C. R., Iwasa, J., Cairns, B. R. & Peterson, C. L. (2017). Mechanisms of action and regulation of ATP-dependent chromatin-remodelling complexes. *Nature Reviews Molecular Cell Biology* Vol. 18, pp. 407–422. doi:10.1038/nrm.2017.26
- Davidson, E.H. (2006). *The Regulatory Genome: Gene*. New York: Academic.
- Donaldson, L. W., Petersen, J. M., Graves, B. J. & McIntosh, L. P. (1996). Solution structure of the ETS domain from murine Ets-1: a winged helix-turn-helix DNA binding motif. *Embo Journal* Vol. 15(1), pp. 125-134. doi:10.1002/j.1460-2075.1996.tb00340.x
- Egger, G., Liang, G., Aparicio, A. & Jones, P. A. (2004). Epigenetics in human disease and prospects for epigenetic therapy. *Nature* Vol. 429(6990), pp. 457-463. doi:10.1038/nature02625.
- Erdel, F., Krug, J., Längst, G. & Rippe, K. (2011). Targeting chromatin remodelers: signals and search mechanisms. *Biochimica et Biophysica Acta - Gene Regulatory Mechanisms* Vol. 1809(9), pp. 497-508. doi:10.1016/j.bbagr.2011.06.005
- Evan, G. (1991). Regulation of gene expression. *British Medical Bulletin*, Vol. 47, pp. 116 - 135.
- Gangenahalli, G. U., Gupta, P., Saluja, D., Verma, Y. K., Kishore, V., Chandra, R., Sharma, R. K. & Ravindranath, T. (2005). Stem Cell Fate Specification: Role of Master Regulatory Switch Transcription Factor PU.1 in Differential Hematopoiesis. *Stem Cells and Development* Vol.14(2), pp. 140-152. doi:10.1089/scd.2005.14.140
- Gibson, D. G., Young, L., Chuang, R. Y., Venter, J. C., Hutchison, C. A. III & Smith, H. O. (2009). Enzymatic assembly of DNA molecules up to several hundred kilobases. *Nature Methods* Vol. 6, pp. 343–345. doi:10.1038/nmeth.1318
- Gupta, P., Gurudutta, G. U., Saluja, D. & Tripathi, R. P. (2010). PU.1 and partners: regulation of haematopoietic stem cell fate in normal and malignant haematopoiesis. *Journal of cellular and molecular medicine Nov - Dec* Vol. 13(11-12), pp. 4349 - 4363. doi:10.1111/j.1582-4934.2009.00757.x
- Gushin, D.Y., Waite, A.J., Katibah, G.E., Miller, J.E., Holmes, M.C. & Rebar, E.J. (2010). A rapid and general assay for monitoring endogenous gene modification. *Methods in Molecular Biology* Vol. 649, pp. 247-256 doi:10.1007/978-1-60761-753-2_15
- Gutierrez-Hartmann, A., Duval, D. L. & Bradford, A. P. (2007). ETS transcription factors in endocrine. *TRENDS in Endocrinology and Metabolism* Vol.18(4), pp. 150-158. doi:10.1016/j.tem.2007.03.002

- Handy, D. E., Castro, R. & Loscalzo, J. (2011). Epigenetic Modifications: Basic Mechanisms and Role in Cardiovascular Disease. *Circulation Vol. 123(19)*, pp. 2145–2156. doi:10.1161/CIRCULATIONAHA.110.956839
- Hargreaves, D. C. & Crabtree, G. R. (2011). ATP-dependent chromatin remodeling: genetics, genomics and mechanisms. *Cell Research Vol. 21*, pp. 396–420. doi:10.1038/cr.2011.32
- Heim, R., Prasher, D. C. & Tsien, R. Y. (1994). Wavelength mutations and posttranslational autoxidation of green fluorescent protein. *Proceedings of the National Academy of Sciences of the United States of America Vol. 91(26)*, pp. 12501-12504. doi:10.1073/pnas.91.26.12501
- Hostettler, L., Grundy, L., Käser-Pébernard, S., Wicky, C., Schafer, W. R. & Glauser DA. (2017). The Bright Fluorescent Protein mNeonGreen Facilitates Protein Expression Analysis In Vivo. *G3 (Bethesda) Vol. 7(2)*, pp. 607-615. doi:10.1534/g3.116.038133
- Howard, M. L. & Davidson, E. H. (2004). cis-Regulatory control circuits in development. *Developmental Biology Vol. 271(1)*, pp. 109-118. doi:10.1016/j.ydbio.2004.03.031
- Iurlaro, M., Stadler, M. B., Masoni, F., Jagani, Z., Galli, G. G. & Schübeler, D. (2021). Mammalian SWI/SNF continuously restores local accessibility to chromatin. *Nature Genetics Vol. 53*, pp. 279–287. doi:10.1038/s41588-020-00768-w
- Izzo, A. & Schneider, R. (2016). The role of linker histone H1 modifications in the regulation of gene expression and chromatin dynamics. *Biochimica et Biophysica Acta (BBA) - Gene Regulatory Mechanisms Vol. 1859(3)*, pp. 486-495. doi:10.1016/j.bbagr.2015.09.003
- Jancewicz, I., Siedlecki, J. A., Sarnowski, T. J. & Sarnowska, E. (2019). BRM: the core ATPase subunit of SWI/SNF chromatin-remodelling complex—a tumour suppressor or tumour-promoting factor? *Epigenetics & Chromatin Vol. 12*, p. 68. doi:10.1186/s13072-019-0315-4
- Jannig, W. & Knust, E. (2004). *Genetik*. Stuttgart: Georg Thieme Verlag.
- Jinek, M., Chylinski, K., Fonfara, I., Hauer, M., Doudna, J. A. & Charpentier, E. (2012). A programmable dual-RNA-guided DNA endonuclease in adaptive bacterial immunity. *Science Vol. 337(6096)*, pp. 816-821. doi:10.1126/science.1225829
- Johnson, P. F. & McKnight, S. L. (1989). Eukaryotic transcriptional regulatory proteins. *Annual Review of Biochemistry Vol. 58*, pp. 799-839. doi:10.1146/annurev.bi.58.070189.004055
- Kadoch, C. & Crabtree, G. R. (2015). Mammalian SWI/SNF chromatin remodeling complexes and cancer: Mechanistic insights gained from human genomics. *Science Advances Vol. 1(5)*, p. 5. doi:10.1126/sciadv.1500447
- Kim, J. H., Lee, S-R., Li, L-H., Park, H-J., Park, J-H., Lee, K. Y., Kim, M-K., Shin, B. A. & Choi, S-Y. (2011). High Cleavage Efficiency of a 2A Peptide Derived from

- Porcine Teschovirus-1 in Human Cell Lines, Zebrafish and Mice. *PLoS ONE Vol. 6(4)*. doi:10.1371/journal.pone.0018556
- Klemsz, M. J., McKercher, S. R., Celada, A., van Beveren, C. & Maki, RA. (1990). The macrophage and B cell-specific transcription factor PU.1 is related to the ets oncogene. *Cell Vol. 61(1)*, pp. 113-124. doi:10.1016/0092-8674(90)90219-5
- Lambert, S. A., Jolma, A., Campitelli, L. F., Das, P. K., Yin, Y., Albu, M., Chen, X., Taipale, J., Hughes, T. R. & Weirauch, M. T. (2018). The Human Transcription Factors. *Cell Vol. 172(4)*, pp. 650 - 665. doi:10.1016/j.cell.2018.01.029
- Latchman, D. S. (1997). Transcription factors: an overview. *The International Journal of Biochemistry & Cell Biology Vol. 29(12)*, pp. 1305-1312. doi:10.1016/s1357-2725(97)00085-x
- Lawrence, M., Daujat, S. & Schneider, R. (2016). Lateral Thinking: How Histone Modifications Regulate Gene Expression. *Trends in Genetics Vol. 32(1)*, pp. 42-56. doi:10.1016/j.tig.2015.10.007
- Lee, T. I. & Young, R. A. (2013). Transcriptional regulation and its misregulation in disease. *Cell Vol. 152(6)*, pp. 1237-1251. doi:10.1016/j.cell.2013.02.014
- Leiz, J., Rutkiewicz, M., Birchmeier, C., Heinemann, U. & Schmidt-Ott, KM. (2021). Technologies for profiling the impact of genomic variants on transcription factor binding. *Medizinische Genetik Vol. 33(2)*, pp. 147-155. doi:10.1515/medgen-2021-2073
- Maniatis, T., Goodbourn, S. & Fischer, J. A. (1987). Regulation of inducible and tissue-specific gene expression. *Science Vol. 236(4806)*, pp. 1237-1245. doi:10.1126/science.3296191
- Mashal, R. D., Koontz, J. & Sklar, J. (1995). Detection of mutations by cleavage of DNA heteroduplexes with bacteriophage resolvases. *Nature Genetics Vol. 9*, pp. 177-183. doi:10.1038/ng0295-177
- Masliah-Planchon, J., Bièche, I., Guinebretière, J. M., Bourdeaut, F. & Delattre, O. (2015). SWI/SNF Chromatin Remodeling and Human Malignancies. *Annual Review of Pathology: Mechanisms of Disease Vol.10*, pp. 145-171. doi:10.1146/annurev-pathol-012414-040445
- Minderjahn, J., Schmidt, A., Fuchs, A., Schill, R., Raithel, J., Babina, M., Schmidl, C., Gebhard, C., Schmidhofer, S., Mendes, K., Ratermann, A., Glatz, D., Nützel, M., Edinger, M., Hoffmann, P., Spang, R., Längst, G., Imhof, A. & Rehli, M. (2020). Mechanisms governing the pioneering and redistribution capabilities of the non-classical pioneer PU.1. *Nature Communications Vol.11(1)*, p. 402. doi:10.1038/s41467-019-13960-2
- Moreau-Gachelin, F., Tavitian, A. & Tambourin, P. (1988). Spi-1 is a putative oncogene in virally induced murine erythroleukaemias. *Nature Vol. 331*, pp. 277-280. doi:10.1038/331277a0

- Morgunova, E. & Taipale, J. (2017). Structural perspective of cooperative transcription factor binding. *Current Opinion in Structural Biology* Vol. 47, pp. 1-8. doi:10.1016/j.sbi.2017.03.006
- Morrison, O. & Thakur, J. (2021). Molecular Complexes at Euchromatin, Heterochromatin and. *International Journal of Molecular Science* Vol. 22(13), p. 6922. doi:10.3390/ijms22136922
- Muchardt, C. & Yaniv, M. (2001). When the SWI/SNF complex remodels ... the cell cycle. *Oncogene* Vol. 20, pp. 3067–3075. doi:10.1038/sj.onc.1204331
- Mueller, B. U., Pabst, T., Osato, M., Asou, N., Johansen, L. M., Minden, M. D., Behre, G., Hiddemann, W., Ito, Y. & Tenen, D. G. (2002). Heterozygous PU.1 mutations are associated with acute myeloid leukemia. *Blood* Vol. 100(3), pp. 998-1007. doi:10.1182/blood.v100.3.998
- Müller-Esterl, W. (2018). Kontrolle der Genexpression. In *Biochemie* (pp. 255-266). Berlin, Heidelberg: Springer Spektrum.
- Nishiyama, C., Nishiyama, M., Ito, T., Masaki, S., Masuoka, N., Yamane, H., Kitamura, T., Ogawa, H. & Okumura, K. (2004). Functional analysis of PU.1 domains in monocyte-specific gene regulation. *FEBS Letters* Vol. 561(1-3), pp. 63-68. doi:10.1016/S0014-5793(04)00116-4
- Orphanides, G., Lagrange, T. & Reinberg, D. (1996). The general transcription factors of RNA polymerase II. *Genes and Development* Vol. 10(21), pp. 2657-2683. doi:10.1101/gad.10.21.2657
- Papillon, J. P. N., Nakajima, K., Adair, C. D., Hempel, J., Jouk, A. O., Karki, R. G., Mathieu, S., Möbitz, H., Ntaganda, R., Smith, T., Visser, M., Hill, S. E., Hurtado, F. K., Chenail, G., Bhang, H. C., Bric, A., Xiang, K., Bushold, G., Gilbert, T., Vattay, A., Dooley, J., Costa, E. A., Park, I., Li, A., Farley, D., Lounkine, E., Yue, Q. K., Xie, X., Zhu, X., Kulathila, R., King, D., Hu, T., Vulic, K., Cantwell, J., Luu, C. & Jagani, Z. (2018). Discovery of Orally Active Inhibitors of Brahma Homolog (BRM)/SMARCA2 ATPase Activity for the Treatment of Brahma Related Gene 1 (BRG1)/SMARCA4-Mutant Cancers. *Journal of Medicinal Chemistry* Vol. 61(22), pp. 10155–10172. doi:10.1021/acs.jmedchem.8b01318
- Parsons, D. W., Li, M., Zhang, X., Jones, S., Leary, R. J., Cheng-Ho Lin, J., Boca, S. M., Carter, H., Samayoa, J., Bettegowda, C., Gallia, G. L., Jallo, G. I., Binder, Z. A., Nikolsky, Y., Hartigan, J., Smith, D. R., Gerhard, D. S., Fults, D. W., van den Berg, S., Berger, M. S., Marie, S. K., Shinjo, S. M., Clara, C., Phillips, P. C., Minturn, J. E., Biegel, J. A., Judkins, A. R., Resnick, A. C., Storm, P. B., Curran, T., He, Y., Rasheed, B. A., Friedman, H. S., Keir, S. T., McLendon, R., Northcott, P. A., Burger, P. C., Riggins, G. J., Karchin, R., Parmigiani, G., Bigner, D. D., Yan, H., Papadopoulos, N., Vogelstein, B., Kinzler, K. W. & Velculescu, V. E. (2011). The genetic landscape of the childhood cancer medulloblastoma. *Science* Vol. 331(6016), pp. 435-439. doi:10.1126/science.1198056

- Peterson, C. L. & Herskowitz, I. (1992). Characterization of the yeast SWI1, SWI2, and SWI3 genes, which encode a global activator of transcription. *Cell Vol. 68(3)*, pp. 573-583. doi:10.1016/0092-8674(92)90192-f.
- Phelan, M. L., Sif, S., Narlikar, G. J. & Kingston, R. E. (1999). Reconstitution of a Core Chromatin Remodeling Complex from SWI/SNF Subunits. *Molecular Cell Vol. 3(2)*, pp. 247-253. doi:10.1016/s1097-2765(00)80315-9
- Pierce, B. A. (2012). In *Genetics: a conceptual approach (4th edition)*, pp. 364-367. New York: W.H. Freeman and Company.
- Reese, J. C. (2003). Basal transcription factors. *Current Opinion in Genetics & Development Vol. 13(2)*, pp. 114-118. doi:10.1016/s0959-437x(03)00013-3
- Reisman, D., Glaros, S. & Thompson, E. A. (2009). The SWI/SNF complex and cancer. *Oncogene Vol. 28(14)*, pp. 1653–1668. doi:10.1038/onc.2009.4
- Reisman, D., Sciarrotta, J., Wang, W., Funkhouser, W. K. & Weissman, B. E. (2003). Loss of BRG1/BRM in human lung cancer cell lines and primary lung cancers: correlation with poor prognosis. *Cancer Research*, pp. 560-566. doi:10.1097/00129039-200503000-00011
- Rothenberg, E. V., Hosokawa, H. & Ungerbäck, J. (2019). Mechanisms of Action of Hematopoietic Transcription Factor PU.1 in Initiation of T-Cell Development. *Frontiers in Immunology Vol. 10*, p. 228. doi:10.3389/fimmu.2019.00228
- Sacchetti, A. & Alberti, S. (1999). Protein tags enhance GFP folding in eukaryotic cells. *Nature Biotechnology Vol. 17*, p. 1046. doi:10.1038/14990
- Sack, U., Támok, A. & Rothe, G. (2006). *Zelluläre Diagnostik: Grundlagen, Methoden und klinische Anwendungen der Durchflusszytometrie*. Basel: Karger.
- Schick, S., Grosche, S., Kohl, K. E., Drpic, D., Jaeger, M. G., Marella, N. C., Imrichova, H., Lin, J. G, Hofstätter, G., Schuster, M., Rendeiro, A. F., Koren, A., Petronczki, M., Bock, C., Müller, A. C., Winter, G. E. & Kubicek, S. (2021). Acute BAF perturbation causes immediate changes in chromatin accessibility. *Nature Genetics Vol. 53(3)*, pp. 269–278. doi:10.1038/s41588-021-00777-3
- Schober, M., Rebay, I. & Perrimon, N. (2005). Function of the ETS transcription factor Yan in border cell migration. *Development Vol. 132(15)*, pp. 3493–3504. doi:10.1242/dev.01911
- Sentmanat, M. F., Peters, S. T., Florian, C. P., Connelly, J. P. & Pruett-Miller, S. M. (2018). A Survey of Validation Strategies for CRISPR-Cas9 Editing. *Scientific Reports Vol. 8*, p. 888. doi:10.1038/s41598-018-19441-8
- Sharrocks, A. D. (2001). The ETS-domain transcription factor family. *Nature Reviews Molecular Cell Biology Vol. 2(11)*, pp. 827-37. doi:10.1038/35099076
- Sharrocks, A. D., Brown, A. L., Ling, Y. & Yates, P. R. (1997). The ETS-domain transcription factor family. *The International Journal of Biochemistry & Cell Biology Vol. 29(12)*, pp. 1371-87. doi:10.1016/s1357-2725(97)00086-1

- Snapp, E. (2005). Design and Use of Fluorescent Fusion Proteins in Cell Biology. *Current Protocols in Cell Biology*, pp. Chapter 21, 21.4.1–21.4.13. doi:10.1002/0471143030.cb2104s27
- Soufi, A., Garcia, M. F., Jaroszewicz, A., Osman, N., Pellegrini, M. & Zaret, K. S. (2015). Pioneer transcription factors target partial DNA motifs on nucleosomes to initiate reprogramming. *Cell Vol. 161(3)*, pp. 555-568. doi:10.1016/j.cell.2015.03.017
- Takei, H. & Kobayashi, S. S. (2019). Targeting transcription factors in acute myeloid leukemia. *International Journal of Hematology Vol. 109(1)*, pp. 28-34. doi:10.1007/s12185-018-2488-1
- Tang, L., Nogales, E. & Ciferrie, C. (2010). Structure and function of SWI/SNF chromatin remodeling complexes and mechanistic implications for transcription. *Progress in Biophysics and Molecular Biology Vol. 102(2-3)*, pp. 122-128. doi:10.1016/j.pbiomolbio.2010.05.001
- Voss, T. C. & Hager, G. (2014). Dynamic regulation of transcriptional states by chromatin and transcription factors. *Nature Reviews Genetics Vol. 15(2)*, pp. 69–81. doi:10.1038/nrg3623
- Waddington, C. H. (1942). The epigenotype . *Endeavour Vol. 1*, pp. 18-20. doi:10.1093/ije/dyr184
- Waldo, G. S., Standish, B. M., Berendzen, J. & Terwilliger, T. C. (1999). Rapid protein-folding assay using green fluorescent protein. *Nature Biotechnology Vol. 17*, pp. 691–695. doi:10.1038/10904
- Wang, G. G., Allis, C. D. & Chi, P. (2007). Chromatin remodeling and cancer, part I: covalent histone modifications. *Trends in Molecular Medicine Vol. 13(9)*, pp. 363-372. doi:10.1016/j.molmed.2007.07.003
- Waterland, R. A. (2006). Epigenetic mechanisms and gastrointestinal development. *The Journal of Pediatrics Vol. 149 (5 Suppl)*, pp. 137-142. doi:10.1016/j.jpeds.2006.06.064
- Weirauch, M. T. & Hughes, T. (2011). A catalogue of eukaryotic transcription factor types, their evolutionary origin, and species distribution. *Subcellular Biochemistry Vol. 52*, pp. 25-73. doi:10.1007/978-90-481-9069-0_3
- Will, B., Vogler, T. O., Narayanagari, S., Bartholdy, B., Todorova, T. I., da Silva Ferreira, M., Chen, J., Yu, Y., Mayer, J., Barreyro, L., Carvajal, L., Neriah, D. B., Roth, M., van Oers, J., Schatzlein, S., McMahon, C., Edelmann, W., Verma, A. & Steidl, U. (2015). Minimal PU.1 reduction induces a preleukemic state and promotes development of acute myeloid leukemia. *Nature Medicine Vol. 21(19)*, pp. 1172–1181. doi:10.1038/nm.3936
- Wilson, B. G. & Roberts, C. W. M. (2011). SWI/SNF nucleosome remodellers and cancer. *Nature Reviews Cancer Vol. 11(7)*, pp. 481–492. doi:10.1038/nrc3068

- Wu, J., Lao, Y. & Li, B. (2019). Nuclear actin switch of the INO80 remodeler. *Journal of Molecular Cell Biology* Vol. 11(5), pp. 343–344. doi:10.1093/jmcb/mjy083
- Wu, Q., Lian, J. B., Stein, J. L., Stein, G. S., Nickerson, J. A. & Imbalzano, A. N. (2017). The BRG1 ATPase of human SWI/SNF chromatin remodeling enzymes as a driver of cancer. *Epigenomics* Vol. 9(6), pp. 919–931. doi:10.2217/epi-2017-0034
- Zhang, P., Behre, G., Pan, J., Iwama, A., Wara-Aswapati, N., Radomska, H. S., Auron, P. E., Tenen, D. G. & Sun, Z. (1999). Negative cross-talk between hematopoietic regulators: GATA proteins repress PU.1. *Proceedings of the National Academy of Sciences of the United States of America* Vol. 96(15), pp. 8705–8710. doi:10.1073/pnas.96.15.8705
- Zhang, T., Cooper, S. & Brockdorff, N. (2015). The interplay of histone modifications - writers that read. *EMBO Reports* Vol. 16(11), pp. 1467-1481. doi:10.15252/embr.201540945
- Zhong, H., Takeda, A., Nazari, R., Shio, H., Blobel, G., & Yaseen, N. R. (2005). Carrier-independent Nuclear Import of the Transcription Factor. *Journal of Biological Chemistry* Vol. 280(11), pp. 10675–10682. doi:10.1074/jbc.M412878200

11. Acknowledgment

Mit diesen Zeilen möchte ich mich bei allen Personen bedanken, die mich während der Forschungsarbeit im Labor und in der Zeit des Schreibens motiviert und unterstützt haben.

Mein erster Dank gilt meinem Doktorvater Herrn Prof. Dr. Michael Rehli für die Bereitstellung des Themas und die ausgezeichnete Betreuung während der gesamten Zeit. Die geduldige Beantwortung meiner zahlreichen Fragen, sowie die immer menschliche und freundliche Art werden mir stets in Erinnerung bleiben.

Des Weiteren möchte ich meinem zweiten Berichterstatter Prof. Dr. Wolfgang Dietmaier für die Übernahme dieses Amtes danken.

Außerdem gilt mein Dank der gesamten AG Rehli für die hilfsbereite und kompetente Unterstützung bei meinen Arbeiten im Labor. Insbesondere möchte ich mich bei Jan Bartel für die Unterstützung im Bereich CRISPR/CAS9 bedanken und bei Johanna Raithel und Hanna Stanewsky für die Mithilfe bei zahlreichen Versuchen und die vielen schönen Momente gemeinsam. Ferner möchte ich mich bei meiner ehemaligen Laborkollegin Kathrin bedanken, da ohne sie die Arbeit im Labor „nur halb so schön“ gewesen wäre.

Auch danke ich der AG Edinger für das Durchführen der FACS Analysen und der AG Thomas für die Aushilfe bei Reagenzien.

Ich danke meinen Eltern für die Ermöglichung meines Studiums und die Unterstützung und Motivation während all den Jahren. Ich könnte mir keine besseren Eltern wünschen.

Zu guter Letzt richte ich meinen Dank noch an meinen Max, der mein häufiges Jammern und Klagen ertragen musste und dabei selbst oft zurückgesteckt hat.

12. Lebenslauf

Persönliche Informationen

Name:

Carolin Franziska Ponetsmüller, geb. Stütz

Geburtsdatum:

4. September 1996

Hochschulausbildung

8. Juli 2021

Approbation zur Zahnärztin

02/2021-06/2021

Zahnärztliche Prüfung

10/2018

Zahnärztliche Vorprüfung

03/2017

Naturwissenschaftliche Prüfung

04/2016–07/2021

Studium der Zahnmedizin, Universität Regensburg

Schulische Ausbildung

06/2015

Erwerb der allgemeinen Hochschulreife

09/2006-06/2015

Schyren-Gymnasium, Pfaffenhofen

Ärztliche Tätigkeit

Seit 10/2021

Vorbereitungsassistentin in der Zahnarztpraxis Dr. Martin Gantner, Au i. d. Hallertau

Auslandsaufenthalt

2012/2013

Auslandsaufenthalt an der Michigan City High School, Indiana und damit verbundene Teilnahme am German American Partnership Program (GAPP)